





**MARTIN TIMUSK**

Development and characterization  
of hybrid electro-optical materials



TARTU UNIVERSITY PRESS

The study was carried out at the Institute of Physics, University of Tartu.

The Dissertation was admitted on April 5, 2012 in partial fulfillment of the requirements for the degree of Doctor of Philosophy in physics and allowed for defense by the Scientific Council of the Institute of Physics, University of Tartu.

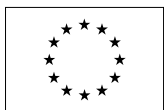
Supervisors: Dr. Kristjan Saal, Institute of Physics, University of Tartu  
Dr. Rünno Lõhmus, Institute of Physics, University of Tartu

Opponents: Dr. Karine Mougin, Institut de Science des Matériaux de  
Mulhouse, University of Haute-Alsace, France

Dr. Mihkel Koel, Department of Chemistry, Faculty of Science,  
Tallinn University of Technology, Estonia

Defence: June 15, 2012 at University of Tartu, Tartu, Estonia

Publication of thesis was supported by: Graduate School on Functional  
Materials and Technologies (GSFMT), University of Tartu and Tallinn Univer-  
sity of Technology, EU Social Funds project 1.2.0401.09-0079



European Union  
European Social Fund



Investing in your future

ISSN 1406-0647

ISBN 978-9949-19-995-2 (trükis)

ISBN 978-9949-19-996-9 (PDF)

Autoriõigus: Martin Timusk, 2012

Tartu Ülikooli Kirjastus

[www.tyk.ee](http://www.tyk.ee)

Tellimus nr. 233

# CONTENTS

LIST OF ORIGINAL PAPERS .....	6
AUTHOR'S CONTRIBUTION .....	7
ABBREVIATIONS .....	8
1. INTRODUCTION .....	9
2. BACKGROUND .....	10
2.1. Electro-optical materials .....	10
2.2. Sol-gel method .....	13
2.2.1. Hybrid materials by sol-gel method .....	15
2.2.2. Methods for tailoring pore size in xerogels .....	17
2.3. Phase separation in sol-gel materials .....	17
2.3.1. Historical overview and theoretical background .....	17
2.3.2. Gel-glass dispersed liquid crystals .....	19
3. GOALS OF THE RESEARCH .....	25
4. EXPERIMENTAL TECHNIQUES .....	26
4.1. Deposition of films .....	26
4.2. Aging of films and preparation of electro-optical devices .....	28
4.3. Film characterization methods .....	29
5. PREPARATION AND CHARACTERISTICS OF GDLC FILMS .....	34
5.1. GDLC films with ormosil matrix (paper I) .....	34
5.2. GDLC films with mixed oxide matrix (paper II) .....	38
5.3. Method of preparation of large area GDLC films (patent) .....	44
6. CONCLUSIONS .....	47
SUMMARY .....	49
SUMMARY IN ESTONIAN .....	50
REFERENCES .....	52
ACKNOWLEDGEMENTS .....	56
PUBLICATIONS .....	57

## LIST OF ORIGINAL PAPERS

- I. M. Timusk, M. Järvekülg, R. Lõhmus, I. Kink, K. Saal, Sol–gel matrix dispersed liquid crystal composite: Influence of methyltriethoxysilane precursor and solvent concentration. *Materials Science and Engineering B*, 172(1) (2010) 1–5.
- II. M. Timusk, M. Järvekülg, A. Salundi, R. Lõhmus, S. Leinberg, I. Kink, K. Saal, Optical properties of high-performance liquid crystal-xerogel microcomposite electro-optical film. *Journal of Materials Research*, 27(9) (2012) 1257–1264.
- III. M. Timusk, M. Järvekülg, K. Saal, R. Lõhmus, I. Kink, A. Lõhmus, Method of preparation of surface coating of variable transmittance and an electro-optical device including the same, Owners: Estonian Nanotechnology Competence Center, University of Tartu, Priority number: P200900022; Priority date: 25.03.2009.

### Other papers in related field:

- IV. M. Järvekülg, R. Vålbe, K. Utt, M. Timusk, T. Tätte, Tailoring Sol-Gel Transition Processes for the Design of Novel Shape Metal Oxide Materials. In: *Functional Oxide Nanostructures and Heterostructures MRS Proceedings Volume 1256E: 2010 MRS Spring Meeting*; San Francisco, USA; 5.–9. April 2010.

## **AUTHOR'S CONTRIBUTION**

The papers and the patent that form the basis of this thesis are the result of collective work with important input and contribution from all of the coauthors with complementary expertise in different fields. The author's contribution to the papers can be described as follows:

- Paper I: Participation in elaboration of synthesis protocols and participation in sol synthesis and film deposition. Post-deposition treatment of films, preparation of electro-optical devices, electro-optical measurements and participation in the analysis of the results. Creating bibliographical background and writing main part of the manuscript.
- Paper II: Participation in elaboration of synthesis protocols and coordination of experimental activities. Participation in the development of the original apparatus for the electro-optical film's field-dependent scattering measurements. Characterization of prepared films, analysis of the results and formulation of key findings. Prevalent part in writing of the manuscript.
- Patent: Participation in elaboration of the patented electro-optical device and method for electro-optical film preparation. Background and novelty search, writing of the part of the patent application.

## **ABBREVIATIONS**

GDLC	Gel-glass dispersed liquid crystal
PDLC	Polymer dispersed liquid crystal
TEOS	Tetraethoxysilane
Me-TES	Methyl triethoxysilane
TIP	Titanium isopropoxide
LC	Liquid crystal
AcAc	Acetylacetone
ITO	Indium tin oxide
SEM	Scanning electron microscope
PVP	Polyvinylpyrrolidone
5CB	4'-Pentyl-4-biphenylcarbonitrile



# I. INTRODUCTION

There is a growing global demand for smart window technologies as these technologies enable the control of solar radiation in building-, automotive- and other applications providing reduced glare and energy efficiency in terms of air conditioning or enable the partitioning of visual space for privacy without the loss of natural illumination. Smart window technologies are a good example of materials engineering moving increasingly from the use and development of passive materials and devices to active materials with tunable properties and enhanced functionality. The two main types of smart window technologies are based on chromogenic- and liquid crystal (LC) dispersion materials. In both classes of these materials reversible change in optical properties can be induced by some external stimulus. Chromogenic materials (either photo-, thermo-, or electrochromic) change light absorption spectrum while the liquid crystal dispersion possesses tunable light scattering.

Liquid crystal dispersions represent a class of electro-optical composite materials, composing of matrix phase dispersed LC microdroplets and possess electric field dependent reversible scattering behavior unique to the composite that is completely absent in the components taken separately. Best known liquid crystal dispersion material is polymer-dispersed liquid crystal (PDLC), consisting of LC microdroplets dispersed in organic polymer. Little known analogue of PDLCs are gel-glass dispersed liquid crystals (GDLCs). GDLC is a hybrid electro-optical film material prepared by a sol-gel method, composing of LC microdroplets encapsulated in inorganic or organically modified silica or mixed oxide matrix. GDLC materials are very little researched – less than 20 scientific papers have been published since they were first reported in 1991. While PDLCs have been in the smart window market for quite some time, despite the great commercial potential no commercial applications exist so far for GDLCs. The reasons behind that for short are the absence of the method of preparation of large area films and poor electro-optical performance, which, at least in principle, could be superior to PDLC in many regards, because the latter has reached its possible limits in performance.

The general goal of this work is to expand the understanding of the formation processes of GDLC, influence of different parameters on GDLC formation, electro-optical characterization of such composite materials and elaboration of a reliable methodology for the preparation of high performance large area GDLC films for the application as a smart window technology. This task is complex and interdisciplinary, requiring completely new precursor sol synthesis protocols and also film deposition method.

## 2. BACKGROUND

The topic of this thesis relates to several distinct fields of research in physics, chemistry and material science. Specifically, the areas involved are electro-optical materials, sol-gel chemistry and -film deposition methods, phase separations in sol-gel systems, liquid crystal dispersions, hybrid inorganic-organic composites, behavior of liquid crystals in confined geometries and Mie-type elastic light scattering. Following these keywords, some essential background information is provided. In the context of the electro-optical materials, PDLCs are briefly described for the reasons that, historically PDLC materials have been mentioned in majority of papers of the GDLC field and these materials are the closest analogs to GDLC materials *by the operating principle* in the field of electro-optical materials. With that the analogy ends. The description of PDLCs enables to provide some essential background information about the relevant properties of the liquid crystals in terms of liquid crystal dispersions. *Structurally* and *by the method of preparation* closest analogs to GDLC materials are not electro-optical materials at all but phase separated macroporous inorganic gels prepared with combined sol-gel and phase separation methods.

### 2.1. Electro-optical materials

Materials that change their optical properties under the influence of electric field are classified as electro-optical materials. The field of electro-optical materials is by no means new. The induced birefringence in the isotropic liquid through the macroscopic alignment of polarizable molecules proportional to the square of the electric field strength was discovered in 1875 by John Kerr and similar effect where field-induced birefringence is proportional to strength of the electric field was discovered by Friedrich C.A. Pockels in 1893. Since that time, as electro-optical effects in some liquids and crystals became known, the variety of electro-optical materials have expanded significantly and include different organic composites [1–4], organic nanocomposites [5,6], hybrid composites [7–9], crystals [10], liquids and solutions of liquids [11], microemulsions (including solid microemulsions) [12–16]. The change of optical properties under the influence of electric field occurs mainly by induced/modified birefringence but change in absorption spectrum can also be induced [17,18]. Good examples of this are electrochromic materials [19,20], in which the change of optical properties relies upon the change of absorption spectrum.

Polymer dispersed liquid crystals were first reported in 1985 [21] and expanded the variety of electro-optical materials and due to a number of potential applications created wide scientific and commercial interest. PDLC is a subclass of liquid crystal dispersion films, composing of organic polymer matrix and liquid crystal (LC) microdroplets randomly dispersed in it. The common methods of preparation are three phase separation techniques; the phase

separation is induced either by polymerization, temperature, or solvent evaporation [22]. As a rule, nematic liquid crystals and their mixtures are used in PDLCs [23] but also successful uses of cholesteric liquid crystal [24] and ferroelectric liquid crystals in PDLC [25,26] have been reported.

Nematic phase is the simplest of spontaneously occurring LC phases in which rod-shaped LC molecules (mesogens) possess long-range orientational order with their longer axis approximately parallel but no long-range translational order [27]. In other words, the disposition of the centers of gravity of individual molecules is random along the axis of long-range order.

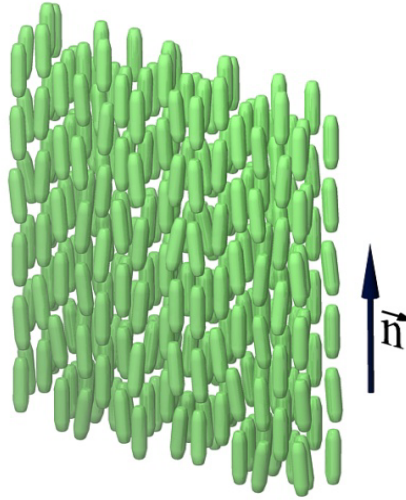


**Figure 1.** Schematic representation of molecular order in nematic LC phase.

PDLC materials strongly scatter light in visible range in their normal state and increase their optical transmittance (decrease scattering) when electric field of sufficient strength is applied, typically becoming more transparent. In practice this is achieved by placing the composite film in between two transparent conductive electrodes (usually indium tin oxide (ITO)). In the field of liquid crystal dispersions, the term “transmittance” has slightly different meaning than usual. The light absorption in these materials can be considered negligible; the change in transmittance means the change in the light scattering.

The operating principle of the material relies on the dielectric and optical anisotropy of LC inside the microdroplets. Nematic liquid crystals as uniaxial optically anisotropic materials exhibit different refractive indices between the two principal values,  $n_e$  – extraordinary refractive index and  $n_o$  – ordinary refractive index, depending on the polarization and the direction of incident light. If the incident light is linearly polarized parallel to the optical axis (extraordinary ray) the refractive index is  $n_e$  and when incident light is polarized perpendicular to the optical axis (ordinary ray) the refractive index is  $n_o$ . In

nematic liquid crystals the optical axis (single direction of propagation along which double refraction does not occur) coincides with the director. The index of refraction for both polarization directions is  $n_o$  along this axis. LC director is a dimensionless unit vector  $\mathbf{n}$  that describes the direction of preferred orientation of molecules in the neighborhood of any point (see Figure 1).

In undeformed LC the director points in the same direction throughout the sample but in small LC droplets, due to the confined geometry, splay, twist, and/or bend deformations arise in liquid crystal with corresponding characteristic elastic constants [28]. The uniform director alignment is distorted, director changes its direction from point to point and the LC possesses a specific director field configuration with a specific effective refractive index  $n_{eff}$  ( $n_e \geq n_{eff} \geq n_o$ ), different from that of the matrix in which the liquid crystal droplets are dispersed in. In this state incident light refracts/scatters at the droplet-matrix boundary due to the mismatch of refractive indices of two phases. As electric field is applied, due to the positive dielectric anisotropy the LC director aligns parallel to the direction of electric field (thermal fluctuations left aside). Consequently, the effective refractive index  $n_{eff}$  of the LC becomes equal to ordinary refractive index  $n_o$  and in the case the matrix material is chosen so that the refractive index of the matrix  $n_m$  equals  $n_o$  of the LC, there is no mismatch of refractive indices and material is transparent. The schematic representation of PDLC operating principle is shown in Figure 2.

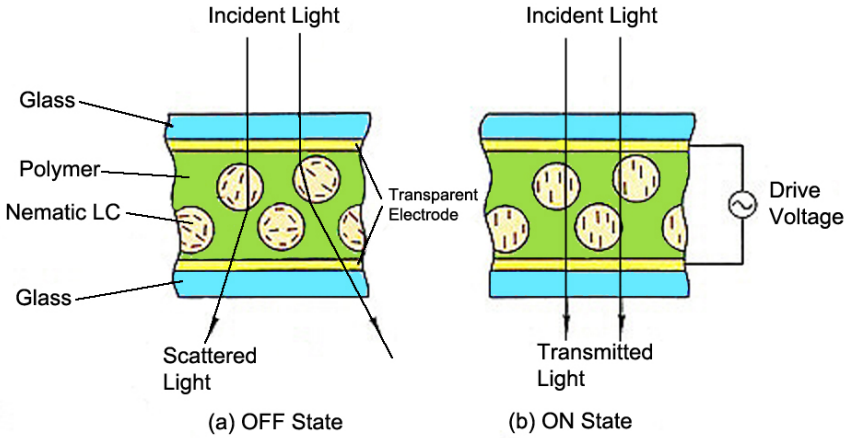


**Figure 2.** A schematic representation of the operating principle of a PDLC device [29].

The electric field strength for switch from scattering to transparent state has been reduced down to 2–5 V<sub>p-p</sub>/μm [4]. Operating voltage, reaction times and optical contrast ratio of the films (the ratio of ON-state transmittance to the OFF-state transmittance) depend on LC droplet size distribution and droplet shape, LC viscosity (temperature), dielectric and optical anisotropy of LC, the anchoring forces on the LC-matrix boundary [4] and dopants inside the LC [30].

Potential applications of PDLC materials include “smart glass” (windows with variable transmittance), optical sensors, light modulators and angular-discriminating filters [31–35].

## 2.2. Sol-gel method

Sol-gel process is a wet chemical method by which the molecular precursors are transformed into an oxide network by hydrolysis and condensation reactions. Commonly the sol-gel synthesis of metal oxides is based on the hydrolysis and polycondensation of metal alkoxides  $M(OR)_z$  in which R is usually an alkyl group ( $R=CH_3, C_2H_5, \dots$ ) and  $z$  the coordination number of the metal atom. The sol-gel process enables to prepare wide variety of structures, including films, fibers, nano- and microparticles and monoliths [36]. Regardless of the form of the prepared structures, the process involves several distinct chemical and non-chemical processing steps which in the case of more widely used hydrolytic sol-gel route are as follows:

1) Liquid alkoxide precursor, such as  $Si(OCH_3)_4$ , is hydrolyzed by mixing with water. Since silicon/metal alkoxides are not miscible with water, alkoxides are commonly dissolved in a co-solvent, usually in parent alcohol, prior to hydrolysis. After alkoxides are mixed with water, two steps of chemical reactions occur [37,38]:



or



The hydrolysis produces the sol. Sols are dispersions of colloidal particles/oligomeric species in a liquid. In reality many factors influence the kinetics of hydrolysis and condensation, and the chemical reactions are considerably more complex than represented by the simplified equations 1–3. Many species are present in the solution and hydrolysis and polycondensation occur to some extent simultaneously. The variables influencing these reactions are temperature, nature and concentration of catalyst (acid, base), nature of the solvent, and type of alkoxide precursor [39]. The complexity of the process is more pronounced in the case of metal alkoxides. Hydrolysis of  $M(OR)_n$  in contrast to hydrolysis of  $Si(OR)_4$  is an extremely fast process, so the main concepts developed for  $Si(OR)_4$  cannot be applied to hydrolysis of metal alkoxides. The electronegativity of metals is lower than that of silicon and unlike silicon alkoxides, metal alkoxide coordination number is often higher than valency. A higher coordination number of metals in their alcoholic derivatives in com-

parison with  $\text{Si(OR)}_4$  leads to high tendency of agglomeration of metal alkoxides in solution prior to hydrolysis as well as to the continuation of this process after first steps of substitution of alkoxy groups by hydroxyl groups in the course of their reactions with water molecules. This results in formation of very complicated oligomeric and polymeric structures [40].

2) Forming of the desired structure (casting the sol into a mold to prepare monolith, preparation of films by spin-coating, dip-coating or spray process, preparation of fibers etc.).

3) Gelation. With time, the colloidal particles and condensed silica species link together, forming a three-dimensional network, or the gel, which is an interconnected rigid network with pores of submicrometer dimensions filled with liquid and polymeric chains whose average length is greater than micrometer. The physical characteristics of the gel network depend greatly upon the size of particles and extent of cross-linking prior to gelation. At gelation, the viscosity increases sharply and a solid object evolves. With appropriate control of the time-dependent change of viscosity of the sol, fibers can be pulled or spun as gelation occurs [39].

4) Aging and drying. These steps can be separate or occur in one step. During aging, polycondensation continues in the material and the strength of the gel increases with aging. Aging is carried out either in closed container without the exposure to ambient humidity, in ambient environment or in liquid environment (sample is immersed in liquid). The separate step of aging is sometimes carried out so that an aged gel would develop sufficient strength to resist cracking during drying. The gel develops into an amorphous micro- or mesoporous xerogel through drying and aging.

According to G.W. Scherer [41,42], the gel cracking occurs as a result of compressive stresses caused by the existence of a meniscus at the liquid–vapor interface as solvents evaporate from the gel pores, which generates a differential capillary pressure and shrinkage of the gel. Shrinkage occurs until material becomes stiff enough to resist the stress imposed by the capillary pressure. The problem of cracking of xerogels is fundamental and the problem is most serious in preparation of thick films and monoliths. Although there may be capillary pressure in the gel, if it were uniform, the network would be uniformly compressed, and there would be no cracking. Therefore, the stress that causes damage results from the pressure gradient across the network and not from the absolute value of the pressure [43]. Several methods have been developed in order to reduce cracking: a) adding drying control chemical additives (DCCAs) to reduce the surface tension of the liquid inside the gel pores [44–46], drying in supercritical conditions [47], increasing the gel pore size by including silica colloid particles in the starting sol [43] using a surfactant (e.g. *n*-octylamine) as a template for the pores in tailoring pore size distribution [48] and incorporating different compounds as additives (such as polyvinylpyrrolidone) in xerogels [49,50]. The list is not exhaustive.

According to Sumio Sakka who is considered as one of the pioneers in the development of sol-gel technology, this technology is a type of nanotechnology since all gel products consist of nanoparticles or nano composites, porous gels contain pores of nano-size diameter, optical gel-solids contain nano-size organic pigments etc. [51].

### 2.2.1. Hybrid materials by sol-gel method

According to J.D. Mackenzie [52] there are two distinct periods of study in sol-gel science. He considers the “birth” of inorganic-organic hybrids from the pioneering work of H. Schmidt in 1985 [53] as one of the two most important advances of sol-gel sciences and technology. Hybrid organic–inorganic materials can be defined as nanocomposites made of organic and inorganic components combined over length scales ranging from a few angstroms to several tens of nanometres. The development of hybrid organic–inorganic materials is mainly due to the development of soft inorganic chemistry processes, especially sol–gel process [54]. Often the “hybrid” is defined as a material that includes two moieties blended on the molecular scale and is divided into two classes: *Class I* hybrid materials are those that possess weak interactions between the two phases, such as van der Waals, hydrogen bonding or weak electrostatic interactions, *Class II* hybrid materials have strong chemical interactions between the components [55].

Since 1985 there has been intense and growing research in this field. The major motivation behind this is the possibility to achieve new and different properties of the nanocomposites which the traditional macroscale composites and conventional materials do not have. Unlike the traditional composite materials which have macroscale domain size of millimeter or micrometer scale, most of the organic-inorganic hybrid materials are nanocomposites with the domain or phase size in the order of 1–100 nm. Such hybrids are often still optically transparent although microphase separation may exist [56].

Organic groups in sol-gel materials can serve different purposes: a) they can control reaction rates of the reactants, rheology of the sols or the homogeneity and microstructure of the gels during the preparation of inorganic materials. In this case they are degraded during calcination to get purely inorganic materials. b) The organic groups can be left inside the material to modify or functionalize the oxide material. In this case, the final material is composed of inorganic oxide structures cross-linked or substituted by organic groups [57].

Hybrid inorganic-organic sol-gel materials can be prepared by two approaches. In the first approach the organic and inorganic parts can be linked by stable chemical bonds. This can be achieved by using alkoxides with functional organic group (an example of organoalkoxysilane is methyl-triethoxysilane (Me-TES)) as precursors in sol-gel process. In general, this approach requires precursors in which the organic group (R) is bonded to the oxide-forming element in a hydrolytically stable way [57]. The materials prepared from these

precursors by sol-gel method are often called ormosils (organically modified silica) and ormocers (organically modified ceramics). The organic groups in inorganic matrix result in the modification of mechanical properties of the material [54,58], modification of surface properties, both surfaces of the pores inside the materials and outer surfaces, in terms of wettability [59,60] and modification of refractive index and porosity [61].

In the second approach for preparing hybrid material by sol-gel method the organic molecules can be just embedded into an inorganic material, or vice versa. This method was pioneered by D. Avnir in 1984 by incorporating organic (dye) molecules into oxide gels [62]. In the case where chemical bonds between inorganic gel network and organic molecules are insignificant, the materials are considered nanocomposites rather than ormosils/ormocers [63].

Both described approaches are important in the context of this thesis. The cited papers (54,58–61) deal with methyl-modified sol-gel materials. The functional methyl groups are also used in this work in preparation of hybrid films. Without the possibility to organically modify amorphous silica- and mixed oxides by the sol-gel method the preparation of GDLC materials would be possible but it would be very difficult to tailor the important operational parameters. In preparation of macroporous hybrid materials by sol-gel method using alkoxides with functional organic groups, the surfaces of the macropores are covered in greater or lesser extent with organic groups (Figure 3). These organic groups determine the behavior of different molecules as they are inserted into the pores.

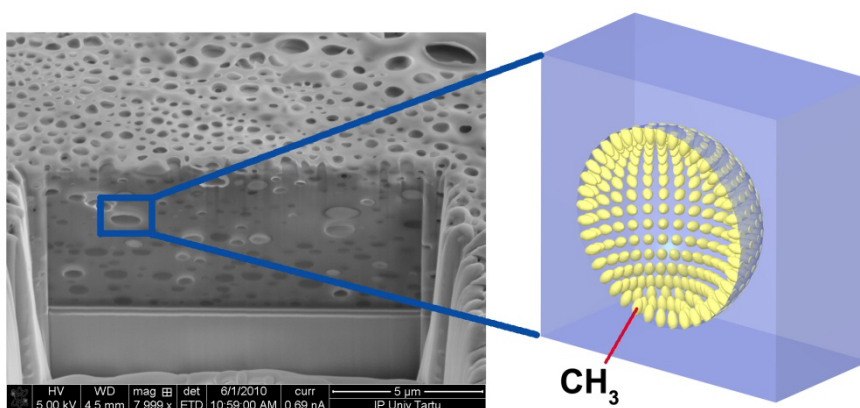


**Figure 3.** SEM image of a macroporous organically modified mixed oxide (left) and a schematic representation of the modification of the pore surface with organic groups.



### 2.2.2. Methods for tailoring pore size in xerogels

As mentioned, precise control over the porosity is necessary to avoid stress-induced cracking caused by differential shrinkage during drying [41], but also for specific pore size distribution to achieve the desired functionality in certain applications. The applications of porous metal- and silicon are wide, including catalysts, photonic crystals, gas and liquid separation membranes, thermal insulation materials, sensors and electro-optical materials [64–69,9]. For the purpose of pore size control, surfactant, emulsion, microsphere colloidal templating and phase separation methods have been used in combination with sol-gel process. These techniques have led to the precise control of the porosity of silicon- and metal oxides at the meso- and macropore ranges in the preparation of hierarchically porous materials with highly versatile and complex morphologies [70–73].

## 2.3. Phase separation in sol-gel materials

### 2.3.1. Historical overview and theoretical background

The phase separation method has emerged as a very powerful means to obtain hierarchically porous oxides with either two co-continuous phases or one fragmented phase inside the continuous micro- or mesoporous matrix phase. The first systematic study of macroporous monolithic silica prepared using the sol-gel phase separation was published in 1991 by K. Nakanishi and N. Soga [74], starting a field of research that has been continuously expanding.

Hydrolysis and polycondensation of alkoxides under acidic conditions gives a relatively narrow distribution of molecular weight of polymerizing oligomers, the average molecular weight of which increases with reaction time. According to thermodynamics of a solution containing polymerizing species, the mutual solubility among components becomes lower as the average molecular weight of the polymerizing species increases. This process reduces entropy of mixing among components and leads to increase of free energy  $\Delta G$  of mixing [75].

$$\Delta G = \Delta H - T\Delta S, \quad (4)$$

where  $\Delta H$  is change in enthalpy,  $T$  – temperature and  $\Delta S$  – change in entropy.

When the sign of  $\Delta G$  becomes positive the phase separation becomes thermodynamically possible. The polymerization reduces the term  $\Delta S$  by decreasing the freedom in chemical configurations. This process can be contrasted to the phase separation in some multicomponent systems (metal alloys, polymer blends etc.) that is achieved by the physical cooling (temperature  $T$  is reduced). In either case the absolute value of the term  $T\Delta S$  decreases. The polymerization can be regarded as “chemical cooling” [73,75]. The difference between physical and chemical cooling is best visible in the respective schematic phase diagrams

in Figure 4. As the number of chemical bonds increases in the sol during polycondensation reaction, the mixture behaves as if the physical temperature is decreased [37]. The phase separation can occur in two different ways, either in the form of nucleation growth or by spinodal decomposition depending on the location of the system in the phase diagram. Between the binodal and spinodal lines the system is metastable and is stable against infinitesimally small fluctuations in composition and density i.e finite activation energy is required to develop phase separated domains. In this state phase separation in the form of nucleation-growth can take place with nucleation occurring on impurities or inclusions. Atoms or molecules diffuse toward nuclei and increase the individual size of the domains, the growth is usually inhomogeneous [73,75,37].

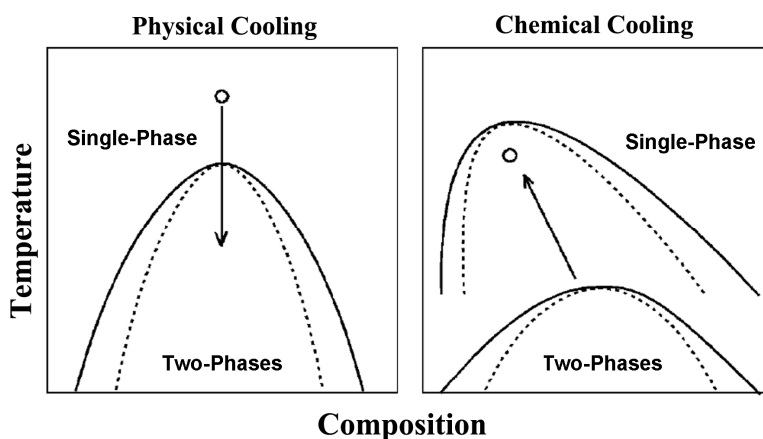


**Figure 4.** Comparison between physical and chemical cooling. The solid and dotted boundaries represent binodal and spinodal lines, respectively. Physical cooling brings a mixture from single-phase to two-phase region by decreasing the temperature. Chemical cooling extends the two-phase region by increasing the number of chemical bonds to include the composition initially located in the single-phase region [37].

Within spinodal line, system is unstable and phase separation in the form of spinodal decomposition occurs (Figure 5). In order to reach the spinodal region in the phase diagram, a transition must occur through the binodal region or through the critical point (point at which binodal and spinodal lines coincide due to the fact that both the first and the second derivative of Gibbs free energy of the system with respect to the composition become zero). Often the phase separation will occur via nucleation during this transition, and spinodal decomposition will not be observed. To observe spinodal decomposition, a very fast „chemical cooling“/polymerization is required to move the system from the stable to the spinodally unstable region of the phase diagram or the transition must occur through the critical point. In the case of spinodal decomposition the

chemical species move against the concentration gradient without an activation barrier and a sponge-like co-continuous structure forms. The structure develops in time through self-similar coarsening driven by interfacial energy. In order to reduce to total interfacial energy the domain structure of the system gets reorganized toward less interfacial area and less local surface energy. The process ultimately leads to fragmentation of domains, given that sol-gel transition has not occurred to that point. The sol-gel transition is a stage in cross-linking polymerization reactions in which steep increase in viscosity occurs and the material turns from viscous fluid to elastic solid. So on one hand polymerization initiates and guides the evolution of phase separation, but on the other hand also freezes it as sol-gel transition is reached as a result of irreversible polycondensation reactions. After the fragmentation of the domains in spinodal decomposition the morphology of the material may closely resemble the structure formed by nucleation growth [73,75,37]

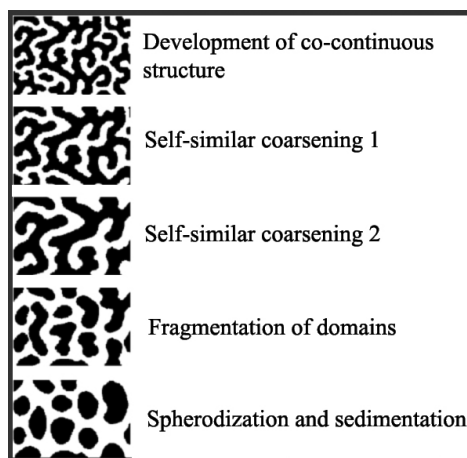


**Figure 5.** Time evolution of a spinodally decomposing isotropic symmetrical system [73]

### 2.3.2. Gel-glass dispersed liquid crystals

Preparation and study of a GDLC material formation is an intrinsic part of the study of phase separation in sol-gel systems, although this connection has never been discussed in papers of the GDLC field. Despite the great commercial potential for the smart window technology, the GDLC materials have been very little researched – in the course of 20 years since a GDLC material was first reported in 1991, less than 20 scientific papers have been published. The ill-defined term “gel-glass” may seem like a bad choice to describe this material but the meaning of this term rather implies to process and stages through which

the material is obtained – sol-gel method, gelation and amorphous structure. The term ODLC (ormosil dispersed liquid crystal) could also be used, but this is limited to cases where only silicon alkoxides are used in the synthesis.

When tetraalkoxysilanes or trialkoxysilanes are hydrolyzed in low  $H_2O/Si$  ratio ( $<2$ ), the siloxane oligomers retain a considerable amount of unreacted alkoxy groups. These oligomers have relatively low polarity and tend to phase separate against highly polar solvent mixtures. In the case of trialkoxysilane like Me-TES the alkoxide has an inherent hydrolytically stable hydrophobic alkyl group that further promotes the phase separation [75,76]. The non-exhaustive list of polar solvents that can be used to achieve phase separation include formamide, dimethylformamide, dimethylsulfoxide, acetonitrile and 4'-pentyl-4-biphenyl-carbonitrile. The latter was first used by Oton *et al.* in 1991 as a polar solvent to achieve phase separation [77,78]. 4'-Pentyl-4-biphenylcarbonitrile (commercially known as 5CB) is a thermotropic liquid crystal in the class of cyanobiphenyls, but in terms of phase separation and formation of the microdroplets this fact has no importance; it is important though in terms of the electro-optical functionality that the material attains after the gel phase is dried and the electro-optical device is prepared. In terms of phase separation the important parameter characterizing 5CB is the value of the dipole moment of 4.87D [79]. 5CB liquid crystal has been used in majority of works in GDLC field since the first work in the field. 5CB is a nematic LC at temperature range from 22.5 to 35.3 C° [79] and has a large positive dielectric anisotropy ( $\epsilon_{||}=18.5$ ,  $\epsilon_{\perp}=7.0$ ,  $\Delta\epsilon=+11.5$  at 25°C) [80] and optical anisotropy. According to Li *et al.* [81] the expressions for dispersion curves of ordinary and extraordinary rays for 5CB at 25°C using three-coefficient Cauchy model are:

$$n_e(\lambda) = 1.6708 + \frac{0.0081}{\lambda^2} + \frac{0.0024}{\lambda^4} \quad (5)$$

$$n_o(\lambda) = 1.5139 + \frac{0.0052}{\lambda^2} + \frac{0.0008}{\lambda^4} \quad (6)$$

where  $n$  – refractive index and  $\lambda$  – wavelength (unit –  $\mu m$ ). From these relations it can be found that at the  $\lambda=589.3$  nm (Fraunhofer D-line)  $n_o=1.536$ ,  $n_e=1.714$ ,  $\Delta n=n_e - n_o=0.191$  ( $T=25^\circ C$ ).

GDLC material is obtained by using LC as a polar solvent in sol-gel process. A GDLC is a hybrid electro-optical material that consists of liquid crystal (LC) microdroplets encapsulated in inorganic or organically modified silica [7,9,82] or mixed oxide matrices [83,84], being essentially a solid microemulsion.

The preparation of GDLC is one of the exceptions among phase separation techniques because it does not include the selective removal of the phase-

separated liquid phase, which is conventionally accomplished in the production of porous materials with a bicontinuous domain structure by phase separation. Instead, the liquid crystal phase is maintained to produce the electro-optical functionality of GDLC.

Similarly to PDLC material, due to the dielectric and optical anisotropy of the LC phase inside the amorphous oxide matrix, the effective refractive index of the liquid crystal microdroplets can be changed relative to that of the oxide matrix. When no electric field is applied, the LCs inside the microdroplets exhibit a complex director field configuration that is determined by the droplet shape, surface anchoring and temperature [85,86]. Depending on the pore surface properties, which, as described in the chapter 2.2.1, can be easily controlled by the proper choice of precursors in the sol-gel process, the molecular alignment of LC at the pore surface can be controlled. The molecules alignment at the pore surfaces in turn propagates over long (macroscopic) distances. For example methyl groups on the pore surfaces induce homeotropic alignment of rod-like LC molecules with the director perpendicular to the droplet boundary which in turn induces radial configuration in the microdroplets, i.e., the liquid crystal director pointing toward the center of the microdroplet at every point [77,86] as shown in Figure 6. Director field configuration control is important since optical characteristics of LC dispersions strongly depend on the latter [87,88]. Large amount of different precursors for sol-gel method provide better flexibility in controlling pore surface properties as compared to PDLC preparation method.

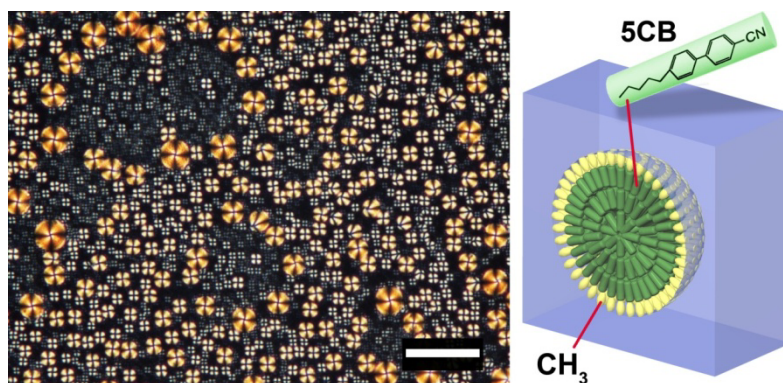


**Figure 6. Left:** Polarized optical microscope image of LC 5CB microdroplets inside organically modified silica. Cross-like patterns under polarized light indicate radial configuration of LC. Scale bar: 15  $\mu\text{m}$ . **Right:** Schematic cross-section of the LC droplet inside methyl-modified matrix. Methyl groups cause homeotropic alignment of rod-like LC molecules with the long molecular axis (director) perpendicular to the droplet boundary from which the radial configuration arises.

As an AC voltage is applied, alternating electric field is induced inside the GDLC film. In a sufficiently strong electric field, the LC molecules tend to align parallel to the field, owing to positive dielectric anisotropy of the 5CB molecules, decreasing the effective refractive index relative to the xerogel matrix and reducing scattering (increasing transmittance). Thus, the material can be switched from an opaque scattering state to a transparent non-scattering state (given that the refractive index of the matrix coincides with the ordinary refractive index  $n_o$  of the LC) by constructing an electro-optical device and applying an electric field in a similar manner to a parallel plate capacitor. However, the dielectric layer between the capacitor electrodes is replaced by microcomposite GDLC film, and transparent conductive films (usually indium-tin oxide) on transparent substrates are used as electrodes. The schematic representation of GDLC operating principle is shown in Figure 7.

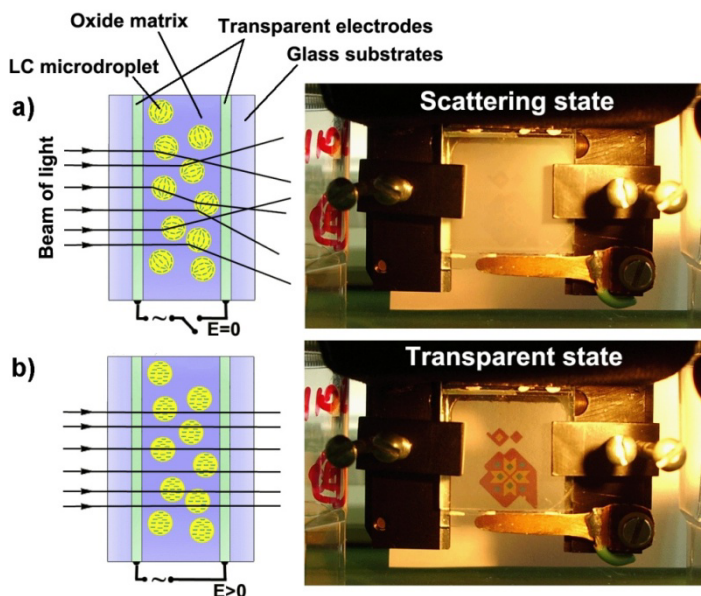


**Figure 7.** Schematic representation of the operating principle of a GDLC electro-optical device. a) When no voltage is applied to the electrodes the effective refractive index of the LC microdroplet differs from that of the oxide matrix and light is strongly scattered. b) AC voltage is applied and alternating electric field is induced between the electrodes. Due to positive dielectric anisotropy, LC molecules tend to align parallel to electric field with the consequent reduction of the effective refractive index. In the case when refractive index of the matrix matches with the ordinary refractive index of the liquid crystal, the material becomes transparent.

Currently there exist several problems concerning the GDLC materials that limit the potential commercial applicability of the material. These problems are listed below. These also summarize well the present state of the GDLC field:

1) The only method used so far for deposition of GDLC films is the spin-coating method. This method enables only to prepare small-area films with relatively low thickness, which is insufficient for effective scattering in field-off state. Spin-coated sol-gel films inevitably possess some center-to-edge thickness variation [89,90]. Additionally, large amount of material is spun off the substrate and goes to waste (up to 98%) [91].

2) The lack of descriptions of the collection optics/collection angle in the transmittance measurements in the papers of the GDLC field makes it is impossible to compare the electro-optical performance of the films reported in different papers. Even more, due to that, no conclusions can be made about the progress in the GDLC field over the past 20 years in terms of the electro-optical performance. The collection angle provides a criterion for discerning transmitted and scattered light. For example, a collection angle of  $\pm 2^\circ$  means that light scattered less than  $2^\circ$  from the direction of incidence is detected as transmitted light.

3) Electro-optical measurements are often performed only at a certain wavelength, using monochromatic light source (such as He-Ne laser,  $\lambda=632.8\text{nm}$ ) [83]. Even with the corresponding information about the collection angle these measurements would only yield very limited information about the films, since the scattering efficiency of a liquid crystal dispersion is wavelength-dependent [87].

3) To achieve high transparency of the GDLC film in the ON-state, the ordinary refractive indices of LC droplets and the matrix must coincide. This condition is relatively difficult to achieve, because the refractive index of applicable LCs is quite high and greatly exceeding that of the organically modified silica. Generally, the higher the content of organic groups, e.g. methyl groups inside the gel/xerogel matrix, the lower the refractive index [61]. Consequently, high performance films cannot be prepared solely from silicon alkoxides and for example transition metal alkoxides must be used instead or in combination with silicon alkoxides to achieve higher refractive index. While high refractive index films have been prepared by sol-gel method for decades, achieving high refractive index of GDLC films without having destructive influence on LC phase separation is a very hard task. Only a few synthesis protocols exist thus far for preparation of GDLC films with the matrix refractive index adjusted to the ordinary refractive index of the LC, but these protocols have serious limitations.

In 1994, Levy *et al.* used titanium isopropoxide (TIP) in the synthesis process but no measurements results of the films containing titanium oxide were presented. It was only stated that addition of TIP resulted in reduced droplet size [92]. An increase in the refractive index was achieved by Chang *et al.* using titanium ethoxide as one of the precursors in the preparation of the sol and preparing the films under low humidity conditions in a glove box [83]. No water was added in the preparation of sol. Instead, titanium ethoxide was added to the mixture of silicon alkoxides and hydrolysis occurred by the influence of

the ambient humidity after the films were prepared. It was not specified though how the films were deposited and the information about the thickness and the area of the films was not provided. Additionally, it was not specified at which collection angle the transmittance measurements were carried out and so, considering these facts, no conclusions can be drawn about the properties of the films.

Hori and Toki [93] used a matrix with high dielectric constant and high refractive index (Ba-Ti-Si oxides) to entrap LC. In this case thin porous films were prepared beforehand and LC was transferred into the pores by vacuum infiltration. Thus, the material obtained by this method is not easily comparable to the GDLC material obtained by the phase separation method. The drawback of this method lies in difficulties in controlling the pore sizes and consequently the electro-optical properties that depend on the latter.

4) No connections have been made between the GDLC field and the large field of the phase separation in sol-gel systems. The GDLC research would potentially benefit from the vast information already available in phase-separation field.



### 3. GOALS OF THE RESEARCH

For the GDLC films to be usable in smart-window applications, the properties of the material must satisfy some important criterions: method of preparation of large area films must be elaborated and the films must exhibit high electro-optical quality. The electro-optical quality (difference between the scattering intensity with and without the applied electric field and effective obscuring the image behind the film in the field-off state) is in turn mainly determined by the film thickness, the LC droplet shape, size distribution and volume density and the magnitude of the mismatch between the refractive index of the matrix and the ordinary refractive index of the LC at a given wavelength. It can be said without a doubt that thus far the state of the art of GDLC materials is still in its infancy (as was also shown in the end of the previous chapter), still being in the proof-of-concept level after 20 years of research. Consequently the general goal of this work is to expand the understanding of the formation processes of GDLCs, influence of different parameters on its formation and electro-optical characterization of such composite materials. This work is necessary in order to move closer to the industrial applicability of GDLC materials as a smart window technology. More specifically the aims of the study were set as follows:

1. Investigation of the possibilities of preparing (both in terms of synthesis and deposition) thick (over 10  $\mu\text{m}$ ), crack-free, high-performance GDLC films. This includes the investigation of formation processes of GDLC materials, influence of different organic modifications and preparation of GDLC films of high refractive index matrix.
2. Determination of the limits of the use of silicon alkoxides in the synthesis process in terms of electro-optical performance of the films.
3. Characterization of prepared films with emphasis on the field-dependent scattering.
4. Elaboration of methods for preparing large area films.

## 4. EXPERIMENTAL TECHNIQUES

The preparation of GDLC electro-optical devices involves several distinct steps. The first step is the synthesis of precursor sols, followed by cleaning/treatment of substrates, deposition of films, aging/annealing and finally, preparation of electro-optical sandwich devices by creating operationally similar devices to parallel plate capacitor where GDLC film acts as (one of) the dielectric layer(s) in between highly transparent electrodes. Following chapters describe the different aspects of preparation and general considerations for the choice of characterization methods chosen for characterizing GDLC films and some key results. Some aspects of the obtained results and applied experimental methods are discussed in more detail in the corresponding papers and patent. For the purpose of better clarity the synthesis of different precursor sols are described in conjunction with the corresponding properties of the resulting films (chapter 5). But first, overview of the deposition techniques and characterization methods is given in Sections 4.1–4.3.

### 4.1. Deposition of films

Despite the significant limitations of the spin-coating method (small area substrates, center-to-edge variation of thickness and coating defects [89,90], difficulty to achieve high thickness, big waste of the deposited material [91]), the GDLC films prepared by spin-coating method are none the less suitable for investigating *some aspects* of the GDLC formation and for investigation of the influence of the composition on its electro-optical characteristics. For that reason the spin-coating method was used, with full understanding of its limitations, as one of the deposition methods in this work. Details of the deposition procedures for preparation of specific films are described in papers I and II ([82] and [84]).

Because of the limitations of the spin-coating method described above, it could not be exploited for realizing one of the main goals of this work, i.e. preparing large area films, so a different method had to be chosen. Another commonly used method for sol-gel film preparation, the dip-coating method, was also disregarded since it is difficult to coat non-planar (curved) substrates (as might be necessary in smart-window applications), technological difficulties in coating large area substrates (a few square meters) and a very large quantity of a precursor sol required for coating which is quite expensive due to the LC that is mixed with the sol. It is also difficult to avoid spoiling of the large amount of sol during the deposition.

For the reasons described above, the spraying method was chosen for films deposition. Spraying method is quite common for preparation of sol-gel films for different applications [94,95], but it must be said that the deposition protocols of GDLC films by spraying method cannot be trivially derived from the information already available in the field. In the case of spin-coating, the deposition step is more

or less independent from the synthesis process, but in the case of preparation of GDLC films by spraying method, spraying stage becomes an integral part of the synthesis process. In order to achieve the desired liquid crystal droplet size distribution in phase separation, that is necessary for effective light scattering at visible wavelength range, solvent evaporation and exposure to ambient humidity in aerosol phase must be taken into account and spraying- as well as synthesis parameters ( $H_2O$ /alkoxide molar ratio, nature and concentration of solvents) very precisely optimized. Otherwise, inappropriate LC droplet size distribution may result or the macroscopic phase separation may not occur at all. In preparation of GDLC films, the sol contains at least two different solvents (LC can be considered a solvent in this regard) with different polarities and vapor pressures. Partial selective evaporation of higher vapor pressure solvents occurs in aerosol phase, in addition to polymerization, adding to the large number of changing variables in the process. So the transition from spin-coating to spray-coating proved to be scientific problem, rather than simply technological one.

The spraying method is not only suitable for coating large surfaces/substrates (e.g. window glasses) with electro-optical films but also allows the preparation of electro-optical films with different 2D patterns (e.g., logos, ads, trademarks, decorations), using masks of corresponding shape during the film deposition process. This is a benefit of spraying method against other deposition methods. A swichable patterned GDLC film, prepared by spraying method is shown in Figure 8.

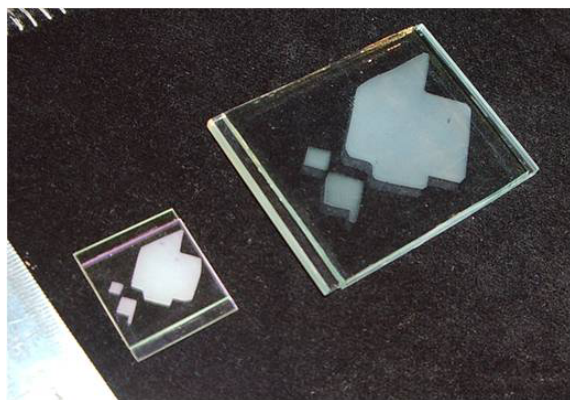


**Figure 8.** Patterned GDLC films prepared by spraying method using masks in deposition process.

The elaborated method of preparation of GDLC films by spraying method and the electro-optical device prepared using this method was patented [96]. The nature of the invention is described in more detail in chapter 5.3.

## 4.2. Aging of films and preparation of electro-optical devices

After the deposition of films onto ITO-covered glass substrates, the samples are left aging either in ambient conditions or in the closed containers for several days and subsequently heated in air (at up to 75°C) to promote solvent evaporation and polymerization reactions. In order to apply electric field to GDLC film, which is necessary in order to change the film's transmittance, a sandwich structures must be prepared in a similar manner to a parallel plate capacitor with GDLC film serving as a dielectric layer between the electrodes. To achieve this, the top electrode, in the form of ITO-coated glass identical to the substrate, is pressed on top of the film with freshly mixed epoxy resin (for example Epotek 310M, Epoxytechnology Inc.) between the film and the top electrode, creating a layered device similar to a parallel plate capacitor. The resin layer, as described above was first used by Levy *et al.* [92] and has not been used since, papers of this thesis excluded. The purpose of the resin layer is to fix the top electrode relative to the film and bottom electrode, to fill a thin residual air gap between the film and the top substrate and to eliminate possible non-switchable light scattering due to the some surface roughness of the film. In addition, high dielectric strength of the resin minimizes the risk of dielectric breakdowns during the operation of the sample. Namely, without resin the applied voltage causes high magnitude electric field in the thin air gap, thus making the device prone to breakdowns due to the low dielectric strength of the air. However, applying the resin virtually eliminates the problem.

It was discovered that as the freshly mixed resin is applied between GDLC film and top electrode, an obvious decrease in scattering occurs in some films. It was found that this effect is caused by the presence of LC droplets that are not completely surrounded by the xerogel matrix, but are open at the film's surface. As resin comes in contact with GDLC film, it dissolves the LC in open droplets or fills the empty droplets as the LC may be evaporated from open droplets during annealing and by that reduces the scattering of the film. High transparency and absence of electro-optical effect results from relatively low thickness of some samples (film thickness close to the diameter of the LC droplet). The existence of open droplets was also confirmed by optical and scanning electron microscopy (SEM) observations (see Figure 9).

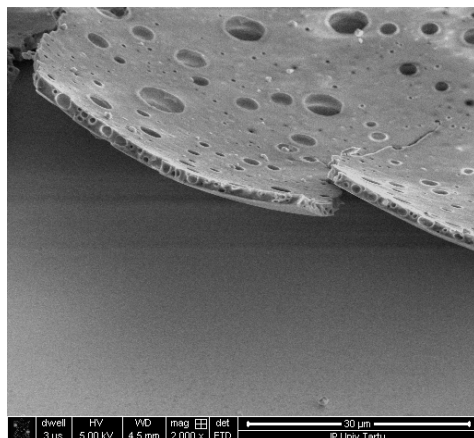


**Figure 9.** SEM image of a surface of the thin (in context of LC dispersion films) GDLC film. The film is cracked and partially detached from the substrate. Layer of open droplets is clearly visible on the surface of the film.

### 4.3. Film characterization methods

Important parameters of GDLC films are LC droplet size (size distribution) and LC director field configuration inside the droplets, film thickness and transmittance dependence on applied voltage.

LC droplet size was determined by optical microscopes Nikon Eclipse 50i Pol and Olympus BX51. Polarized optical microscope enables to some extent to determine the LC director field configuration (as shown in Figure 6.) LC configuration partially determines light scattering efficiency in field-off state. In the case of thick films where several “layers” of droplets exist, individual droplets are hardly discernible and due to strong light scattering that these kinds of films exhibit, optical microscope is not usable for imaging such films and SEM imaging must be preferred in that case.

The thicknesses of the GDLC and resin layers between the ITO electrodes were measured with a Tescan Vega SEM after the device was broken in half along the lines scraped with a diamond tip to reveal the cross-section, washed in methanol and dried in an  $N_2$  gas flow. An example of the cross section of the GDLC electro-optical device is shown in Figure 10.

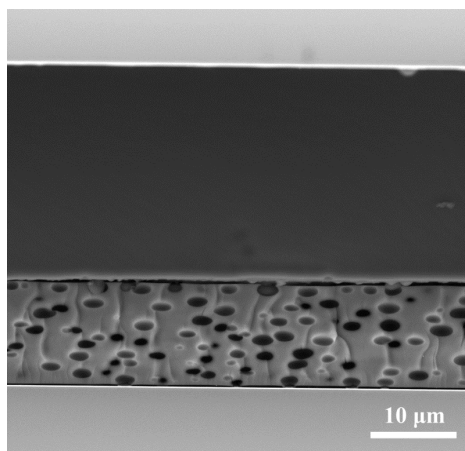


**Figure 10.** SEM micrograph of the cross-section of the electro-optical device consisting of layers (from bottom up) of glass, ITO, GDLC film, resin, ITO and glass. Thickness of the GDLC film is 11.98  $\mu\text{m}$ . The preparation of this film is described in paper II.

In addition to the precise thickness measurements, imaging of the film's cross-section also reveals the true shape of the liquid crystal droplets, which appear to be spherical in optical microscope images taken perpendicular to the film surface. The cross-section image (Figure 10) reveals that the droplets are actually oblate spheroids in shape, with an average aspect ratio (ratio of the minor to major axis length) of 0.476. The shape deviation from oblate spheroid only occurs in close proximity to another droplet or near the film boundaries. In this work the oblate spheroid shape of LC droplets in xerogel matrix is shown for the first time. The geometry of the droplets arises from their initial spherical shape right after the phase separation as they change shape due to the shrinkage during drying as the solvents evaporate. The deformability of the liquid phase prevents stress buildup, which explains why relatively thick films are obtained without cracking or pulverization. Similar phenomenon was also observed by Imhof and Pine, who prepared macroporous sol-gel materials by emulsion templating [71]. This is a significant result since it shows for the first time that thick crack-free GDLC films can be successfully prepared. In the contrast, the critical thickness of sol-gel films (thickness at which cracking occurs) is considered to be about 1  $\mu\text{m}$ , if special measures against cracking are not implemented [47]. High thickness of GDLC films is a necessary requirement for effective scattering in the field-off state and for high contrast ratios of the films (the ratio of ON-state transmittance to the OFF-state transmittance). The oblateness of droplets can be possibly quite easily be controlled by the solvent concentration. The possibility to control the shape of the droplets shows the superiority of GDLC preparation method against PDLC preparation method in this aspect.

The most important characteristic of GDLC films is the transmittance dependence on applied voltage. As said, in GDLC (and also in PDLC materials for

that matter) light absorption is very small and can be neglected for all practical purposes and change in transmittance means change in angular scattering intensity and not the change in light absorption. Light that is scattered less than a certain angle normal to the plane of the film is detected as transmitted light (schematically shown in Figure 11). The transmittance  $T$  is calculated as the ratio of the film transmission intensities (Figure 11 c)) to the reference transmission intensities (Figure 11 a)) at the corresponding wavelengths (Eq. 5).

$$T = \frac{I_t}{I_0} \quad (5)$$

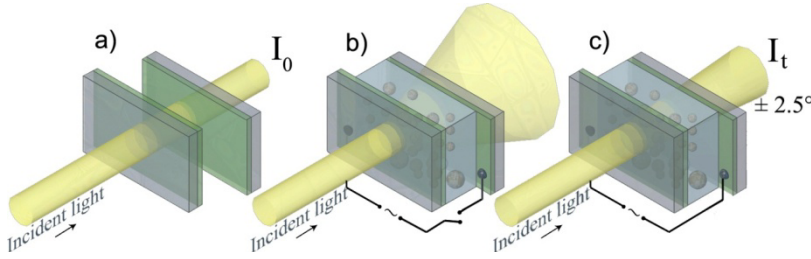


**Figure 11.** General principle of GDLC transmittance measurement. b) As no voltage is applied to GDLC electro-optical device, light is strongly scattered. c) As voltage is applied, scattering is reduced and in the case all the light is transmitted into some small critical solid angle, transmittance of 100% is reached. Transmittance  $T$  is calculated as the ratio of the film transmission intensity  $I_t$  to the reference transmission intensity  $I_0$  (shown in part a)) at the corresponding wavelengths.

As was described in chapter 2, over the years that GDLC materials have been researched transmittance measurements have not correctly been carried out and without the information about the collection angle, measurement results are not correctly interpretable. However, it is known that an arbitrarily high contrast ratio (the ratio of ON-state transmittance to the OFF-state transmittance) can be measured for almost any liquid crystal dispersion film by the choice of collection angle alone [87]. Thus the arbitrary choice of the collection angle can make the poor electro-optical quality films appear as high-quality films judged by the incorrectly measured transmittance vs. applied voltage curves. This in turn may lead to the incredible and incompetent statements that GDLC layers of about 2  $\mu\text{m}$  thickness which is much less than films thickness of PDLCs, which is between 20 and 50  $\mu\text{m}$ , exhibit similar electro-optical responses [9]. This is clearly impossible since scattering efficiency of LC dispersion films depends exponentially on thickness [87].

To correctly evaluate the electro-optical quality of the prepared GDLC films reported in this thesis, a measurement chamber was developed with an optical setup that enables measurements of the transmittance dependence on applied

voltage in a controllable temperature environment, at different frequencies and in wide spectral range. The measurement is made at a  $\pm 2.5^\circ$  collection angle in a wavelength range from 350 to 1100 nm in 0.477-nm increment, using a collimated beam 3 mm in diameter. Slightly different setup was used for measurements in paper I. In this earlier paper [82],  $\pm 2.4^\circ$  collection angle was used as well as a different spectrometer. After that, the setup was improved in order to decrease noise in the measurements, also the collection angle was adjusted to  $\pm 2.5^\circ$  and the scheme as described here was used for measurements in paper II [84]. After the setup was improved, the measurement accuracy was significantly improved. Despite the slightly different collection angle, the results presented in two papers are still quite well comparable in this regard.

The complicated setup consisting of lenses, diaphragms and suitable optical cables is required because the transmittance cannot be correctly measured by a simple setup containing a laser light source and a photodetector placed at a certain distance from the film to obtain a certain collection angle, even if a monochromatic light source is used. From a purely geometrical perspective, it would be possible to use this simple configuration only in the case of an infinitely narrow beam diameter. Because the LC droplet diameters are usually in the order of one micrometer, and the light scattering intensity angular dependence arises statistically from random refractions at the matrix-LC droplet boundary caused by the change in the effective refractive index, the beam diameter must be much larger than the droplet diameter – in the order of a millimeter. For this reason, to achieve the desired collection angle with a wide beam diameter, the more complicated setup is required for the transmittance measurements. The setup that was used for transmittance measurements is schematically shown in Figure 12.

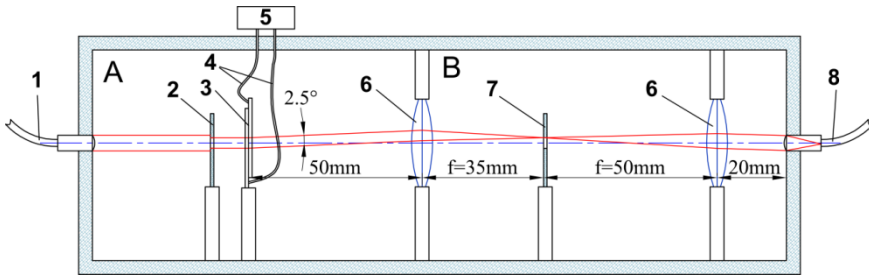


**Figure 12.** Scheme of the setup used for transmittance measurement at  $\pm 2.5^\circ$  collection angle. **1** – optical fiber connecting white light source and collimator lens via SMA 905 connector, **2** – diaphragm  $\varnothing$  3mm, **3** – sample (GDLC electro-optical element) (see also Figure 9), **4** – wires through which the voltage is applied to the sample, **5** – AC voltage generator, **6** – high quality optical lenses, **7** – diaphragm  $\varnothing$  3.056mm, **8** – optical cable with 600  $\mu$ m core diameter, connecting spectrometer and collimator lens via SMA 905 connectors.



White light source (Ocean Optics LS-1 with 10000 h bulb) and a spectrometer (Ocean Optics HR2000+ES) were used in transmittance measurements. The reference spectrum, which is necessary for the calculation of the transmittance, was averaged from 10 measurements that were acquired using two ITO substrates sandwiched together with Epotek 310M resin to obtain a similar layered structure to the GDLC device, except for the presence of the GDLC film. Then, the transmission spectrum of the GDLC device was measured by applying a square wave AC voltage (Metrix mtx3240 signal generator) to the film through a voltage amplifier. A 1 s queue time was set between the gradual increase of the voltage and spectrum acquisition to ensure sufficient response time for the LCs. The voltage on the ITO electrodes was measured with an Agilent 34410A multimeter. At each voltage value, the spectrum was measured 10 times and averaged. The operation of all devices was synchronously controlled by a PC using a Labview program, developed for that purpose.

## **5. PREPARATION AND CHARACTERISTICS OF GDLC FILMS**

### **5.1. GDLC films with ormosil matrix (paper I)**

Several different approaches were used in the precursor sol synthesis with different specific goals. The first approach (described in detail in paper I, [82]) included the preparation of sol using two silicon alkoxides (tetraethoxysilane (TEOS) and methyltriethoxysilane (Me-TES)) in different molar ratios (from 5:1 to 1:5) which resulted in organically modified silica matrix of the GDLC films with different concentrations of methyl groups. The use of trialkoxy-(alkyl)silane (in this case Me-TES) serves several purposes in the context of this work. Methyl groups remain inside the matrix and on the matrix-LC boundary, determining surface anchoring forces [9]. Due to the confined geometry, splay, twist, and/or bend deformations arise in liquid crystal with corresponding characteristic elastic constants that decrease with increasing temperature [28]. The LC director field configuration arises as an equilibrium condition between elastic forces and the forces on the orienting boundary. So in short, the organic groups on the droplet boundary influence the operating voltage of the GDLC device through surface anchoring forces, and scattering properties through LC director field configuration. Additionally, as was described in section 2.3.2, the hydrolytically stable hydrophobic alkyl groups promote phase separation against highly polar solvent [75,76]. Different trialkoxy(alkyl)silanes can be potentially used instead of Me-TES.

The goals and new approaches of paper I were:

- To investigate the influence of organic modification to different extents by methyl groups on the properties of the film.
- To investigate the possibility of carrying out the synthesis of the sol without the solvents in the synthesis process and possible benefits of such approach.
- To determine whether polyvinylpyrrolidone (PVP) can be successfully added without the negative influence on the formation of the film morphology. PVP is known to be a preventive measure against sol-gel materials cracking upon gelling [49,50], but in the context of preparation of GDLC films it is used for the first time.

The measurement results are presented on the following figures (Figures 13–15).

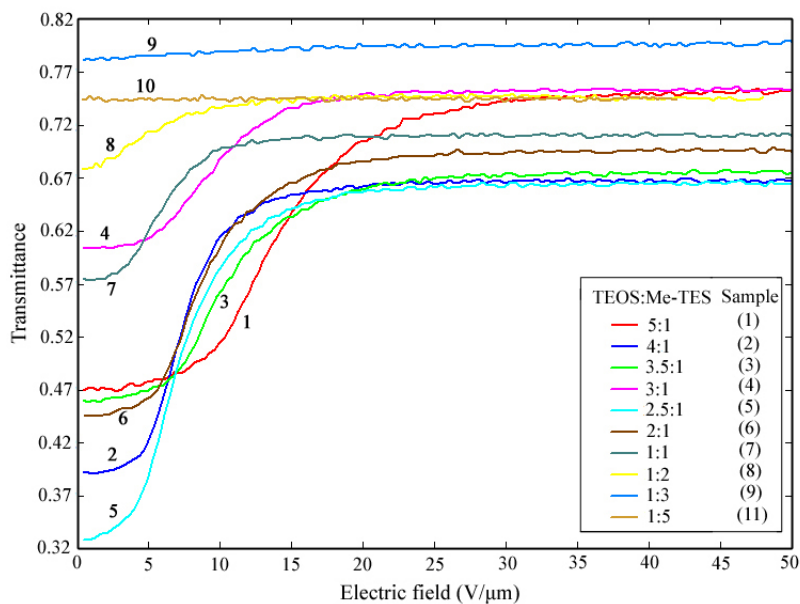


**Figure 13.** Transmittance vs. applied electric field at 633nm for series prepared with ethanol.

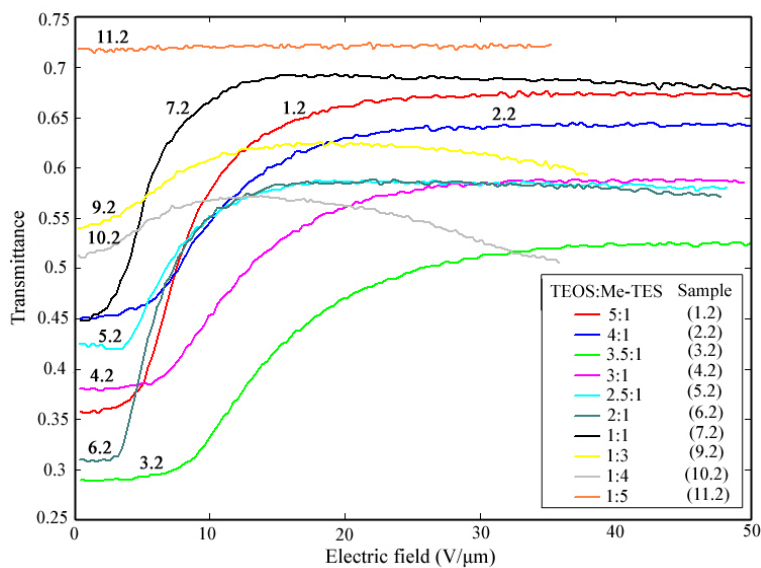


**Figure 14.** Transmittance vs. applied electric field at 633nm for series prepared without ethanol.

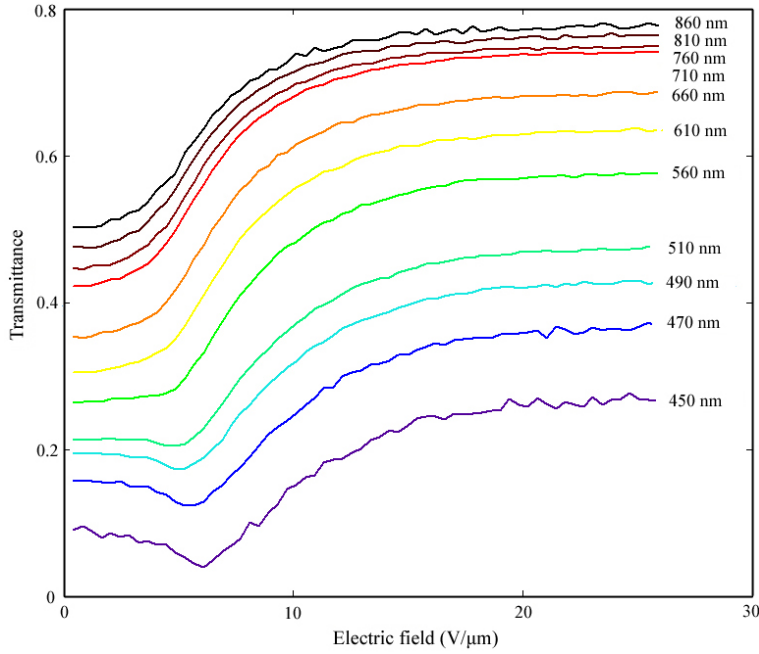


**Figure 15.** Dependence of transmittance on applied electric field at different wavelengths performed on sample 5 (TEOS : Me-TES ratio of 2.5:1 from series of films prepared with solvent).

Key results and conclusions of paper I were:

- It was found that LC phase separation may occur in such a way that a certain percentage of LC droplets are not completely surrounded by gel-glass matrix, but are open on the film surface.
- Due to the layer of open droplets, applying of resin possesses a deteriorating effect on the scattering efficiency of the film as resin fills the open droplets, consequently the the part of the thickness of the GDLC film that contributes to the reversable scattering and what could be called the effective thickness, may be up to 2–3 $\mu\text{m}$  smaller than the total/physical thickness, depending on the LC droplet size distribution. By developing means to reduce the formation of open droplets, the effective thickness can be increased without increasing the physical thickness. The resin layer is necessary to avoid dielectric brakedowns and to eliminate scattering by the surface roughness.
- If was found that different concentration of methyl groups influence the gelation time and by that the droplet size distribution. Thus it can be concluded that the operating voltage is not directly influenced solely by the molar ratio of the precursor alkoxides, but by the difference in droplet size distribution originating from it. In case of investigating the influence of different functional groups (ethyl, propyl, butyl groups), samples with

identical droplet size distribution have to be studied in order to yield directly comparable operating voltages.

- Possibility of preparing ODLC films without adding solvent in the sol synthesis stage was shown for the first time. Homogeneous sols can be prepared from silicon alkoxides by mixing them directly with acid-water solution. Although some alcohol (approximately 3–4 moles per 1 mole of alkoxide) is created by chemical reactions during ODLC formation, it was shown that generally, avoiding solvents in the process results in wider LC droplet size distribution, increased thickness of films, and larger variation of the transmittance.
- The sample with the biggest change in transmittance  $\Delta T$  (at 633 nm) in series prepared with ethanol had TEOS: Me-TES ratio of 2.5:1 with change in transmittance  $\Delta T=33.9\%$ , and in series prepared without ethanol had TEOS:Me-TES ratio of 5:1 with  $\Delta T=31\%$ . Although the biggest change in transmittance occurred in the sample prepared with the use of solvent, the general trend was that samples prepared without solvent exhibited bigger changes in transmittance as compared to the samples prepared with solvent.
- Adding PVP did not have destructive influence on the formation of the film morphology and thus can be successfully used as one of the preventive measures against cracking.
- An unexpected but clear tendency was observable in three samples (7.2, 9.2 and 10.2, Figure 13) that were prepared without solvent. Instead of reaching a plateau, the transmittance declined at high electric field strengths. Effect grew progressively stronger from samples 7.2 to 10.2, the transmittance of the latter sample decreased to a value that was lower compared to the transmittance at field-off state. Identical effect was observed when the experiments were repeated. The cause of this effect is currently unknown.
- Transmittance of sample 5 at different wavelengths (Figure 15) shows increasing operating voltage at shorter wavelengths. This result is expected since smaller droplets scatter light more effectively at shorter wavelengths, while certainly require higher electric field to reorient LC molecules inside the droplets. Absolute change of transmittance had a maximum value of  $\Delta T=33.9\%$  at 660 nm and decreased towards both shorter and longer wavelengths ( $\Delta T=24.4\%$  at 450 nm and  $28.2\%$  at 860 nm). As the wavelength was increased considerable shift of curves in the direction of higher transmittance values could be seen. Initial transmittance (at zero field) varied significantly with wavelength.
- Generally, the prepared films exhibited relatively poor electro-optical performance, attributable to insufficient thickness (the thickest obtained film was 3.8  $\mu\text{m}$  thick), deteriorating effect of the resin and low refractive index of the matrix the value of which for the films with similar composition cannot exceed 1.44 (at 630 nm) according to the literature data [61].

## 5.2. GDLC films with mixed oxide matrix (paper II)

From the results described in the paper I it was clear that different approach for the synthesis was needed and more thorough characterization of films was necessary. Although the focus of the paper II is not on the synthesis, the new synthesis protocol is presented to yield high-performance films. The goals set in the paper II were:

- To investigate the field-dependent scattering behavior of a refractive index-matched GDLC film over a broad spectral (from visible to near-IR) and temperature range. The performance of GDLC films at different temperatures is very important in terms of potential practical applications as is the scattering behavior at different wavelengths, which determines the effective obscuring of the image behind the film.
- To propose a method to characterize the electro-optical quality of GDLC films integrally, based on the measurement of changes in their transmittance over a wide spectral range and by that, to provide a necessary basis for the future development of GDLC materials.
- Elaboration of synthesis protocol for preparation of high-performance films.

In the elaboration of sol synthesis protocol, the goal was set to prepare GDLC film with mixed silicon-titanium alkoxide precursor derived matrix. The TEOS, Me-TES and titanium isopropoxide (TIP) were chosen as precursors in sol synthesis. The synthesis is described in detail in paper II. In short, the synthesis was carried out in two parts. Part A consisted of the classical hydrolytic sol-gel process with an acid catalyst where TEOS, Me-TES and isopropyl alcohol were mixed in a given order at room temperature at molar ratios of 0.55:0.3:0.4. A 0.343 M  $\text{HNO}_3$  aqueous solution was added dropwise to the silane-alcohol mixture on a magnetic stirrer to yield R ( $\text{H}_2\text{O}/\text{alkoxide}$  molar ratio) = 1.45. Part B: Acetylacetone (AcAc) was added dropwise to titanium isopropoxide on a magnetic stirrer at room temperature at a 1:1 molar ratio to obtain Ti-acetylacetonate. Part A and part B were allowed to react separately for 2 hours and then mixed to obtain a Ti/Si atomic ratio of 0.2. Because of the significantly higher hydrolysis and polycondensation rates of titanium alkoxides compared to silicon alkoxides [97], acetylacetone is commonly used as chelating agent to reduce the reaction rates of titanium alkoxides [54,97–99]. The enolic form of acetylacetone contains hydroxyl groups, which react readily with titanium alkoxides to yield a corresponding alcohol and a modified alkoxide precursor [100]. If the difference in the reaction rates of the precursor compounds is not adequately addressed, macroscopic phase separation is hindered by rapid gelation and will probably also accompany an inhomogeneous distribution of titanium inside the film as a result of the homocondensation of the titanium compounds [101]. The mixture of parts A and B was homogeneous and clear, with a yellowish color because of the Ti-acetylacetonate. The sol was stirred for 15 minutes after mixing parts A and B and mixed with LC 4-cyano-4'-pentylbiphenyl at a 10:1 volume ratio which resulted in clear homogeneous solution that at this stage was ready for deposition.

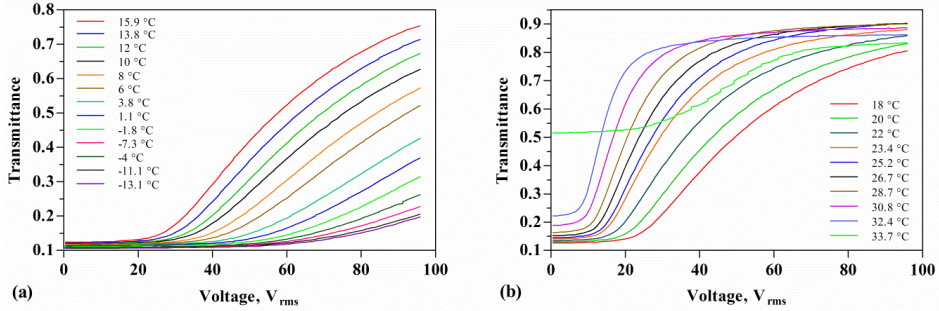
The optimal Ti/Si ratio in terms of refractive index may be slightly different though than was used in the paper. But from the fact that this ratio enables to achieve transmittances over 90% in thick film as was evident by the measurements, this ratio is close to optimal and was considered sufficient in the context of this study. It was clear though that for the experiments to be systematic, the refractive index measurements were necessary. Extensive experiments were carried out to determine the matrix material's refractive index (dispersion curve) dependence on Ti/Si ratio. Unfortunately, all of these experiments were unsuccessful and thus were excluded from the paper. Several series of films with varying Ti/Si ratio were deposited onto silicon wafers for refractive index measurements by ellipsometry. Since the films were amorphous, organically modified and with high porosity, sufficiently accurate fit to the experimental data could not be made. Also, possibility of refractive index measurements from film's transmission spectrum was explored using the Swanepoel method [102]. This too proved to be unsuccessful due to the difficulties to satisfy the presumptions of this approach (very low absorption in substrate etc.). Reliable method for film's refractive index measurement must be found in the future as the work continues.

The GDLC film that is incorporated into electro-optical device investigated in paper II is shown in Figure 10. The film thickness is 11.98  $\mu\text{m}$  which is considerably thicker than the film thicknesses reported in paper I. This can be attributed to lower rotation speed in deposition, higher viscosity and different wettability properties of the sol. Although relatively thin films are usually prepared by spin-coating method, films with thickness of up to 25  $\mu\text{m}$  in single coating cycle have been reported [103]. This of course does not mean that high thickness is achievable using just any sol. Sols with different composition can have very different properties.

One of the important results of paper II is that thick, crack-free GDLC films can be successfully prepared. The absence of cracking can be attributed to the deformability of the liquid phase that prevents stress buildup as was discussed in chapter 4.3.

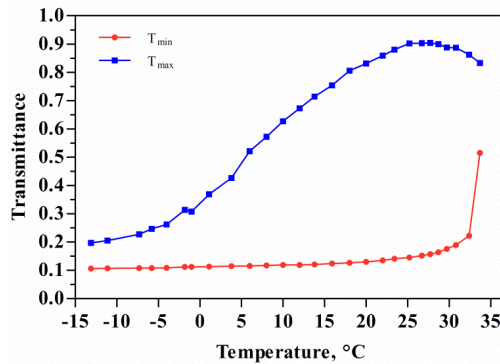
The measurements of field-dependent scattering behavior in broad spectral (from visible to near-IR) and temperature range were carried out. From these measurements, the transmittance vs. the applied voltage at 1572 different wavelengths from 350 to 1100 nm was obtained at 27 different temperatures (between -13 °C and 33 °C). From this data set, several relations were found: a) the evolution of the transmittance  $T$  vs. applied voltage  $U$  at 550 nm wavelength with increasing temperature, b) the evolution of the change in transmittance ( $\Delta T = T_{\text{max}} - T_{\text{min}} = T_{95V_{\text{rms}}} - T_{1V_{\text{rms}}}$ ) vs. wavelength ( $\lambda$ ) with increasing temperature, c) the maxima of the  $\Delta T$  vs.  $\lambda$  graph vs. temperature, d) the area under the  $\Delta T$  vs.  $\lambda$  curve in the visible range vs. temperature, e) the  $\Delta T$  vs.  $\lambda$  graph evolution with increasing voltage (measured at a temperature of 25.2 °C) and f) the area under the  $\Delta T$  vs.  $\lambda$  curve in the visible range vs. applied voltage (given at a temperature of 25.2 °C since maximum change in transmittance occurs at that temperature).

Figure 16 presents the evolution of the dependence of the transmittance on the applied voltage at  $\lambda=550$  nm with increasing temperature. The data set is presented in two parts for better clarity: Figure 14 a) depicts the dependence of the transmittance on the applied voltage in the temperature range from  $-13.1$  °C to  $15.9$  °C and Figure 14 b) shows the temperature range from  $18$  °C to  $33.7$  °C.



**Figure 16.** Evolution of the transmittance dependence on the applied voltage at  $\lambda=550$  nm with increasing temperature from  $-13.1$  °C to  $15.9$  °C a) and from  $18$  °C to  $33.7$  °C b).

Several observations can be made from Figure 16. Notably, the operating voltage increases significantly with decreasing temperature. The transmittance saturation plateau, for which increasing voltage does not induce an increase of the transmittance, is reached only at approximately  $29$  °C. It can also be observed that both  $T_{min}$  and  $T_{max}$  increase with increasing temperature, up to a temperature of approximately  $25.2$  °C, at which  $T_{min}$  continues to increase with increasing temperature but  $T_{max}$  begins to decrease.  $T_{min}$  and  $T_{max}$  as functions of temperature are presented in Figure 17.



**Figure 17.**  $T_{min}$  and  $T_{max}$  as functions of temperature at  $\lambda=550$  nm.



It can be deduced from Figure 17 that  $\Delta T \rightarrow 0$  as the temperature approaches the nematic-isotropic transition temperature of 35.3 °C. It can also be observed that a strong electro-optical effect exists well below the nematic range of 22.5–35.3 °C [79], at least down to –13 °C. This supercooling effect is known to occur inside small pores due to disordering influence of pore surface and random pore structure, inducing glass formation rather than crystallization far below nematic-crystal bulk phase transition temperature [104,105]. This is an important property for the practical applications where 5CB is used as a pure compound instead of a eutectic mixture of different liquid crystals, allowing GDLC electro-optical device to operate below the solid-nematic phase transition temperature.

As the change of transmittance  $\Delta T$  is plotted against wavelength (Figure 18), it can be observed that the change in the transmittance is strongly wavelength dependent, and a curve with a distinct maximum evolves with increasing temperature in a complicated way. For this reason, measuring the transmittance at a single arbitrary wavelength yields inconclusive information about the scattering properties of the film. In this graph, each point on the curve represents a datum contained in the transmittance vs. applied voltage curve in the form of the  $T_{min}$  and  $T_{max}$  ( $\Delta T = T_{max} - T_{min}$ ) values at a certain wavelength. At low temperatures, a large change in transmittance occurs in the IR region, while  $\Delta T$  is relatively small in the middle of the visible range. As the temperature increases, the maximum of the curve moves progressively toward shorter wavelengths, and  $\Delta T$  achieves a maximum value of 75.9% at 25.2 °C and 551 nm. As the temperature increases further (Figure 18 b)),  $\Delta T$  begins to decrease, while the maximum of the curve continues to move toward shorter wavelengths. The achieved change of transmittance is sufficient for practical applications both by observing film's switching behavior visually and also judged by the measurements. In 1999, Nicoletta *et al.* stated that PDLCs with an ON-state transmittance of 80% and an OFF-state transmittance less than 2% are considered good industrial standards for a reasonably small collection angle like 2.5° [106]. This gives a good basis for comparison with results presented in this thesis.

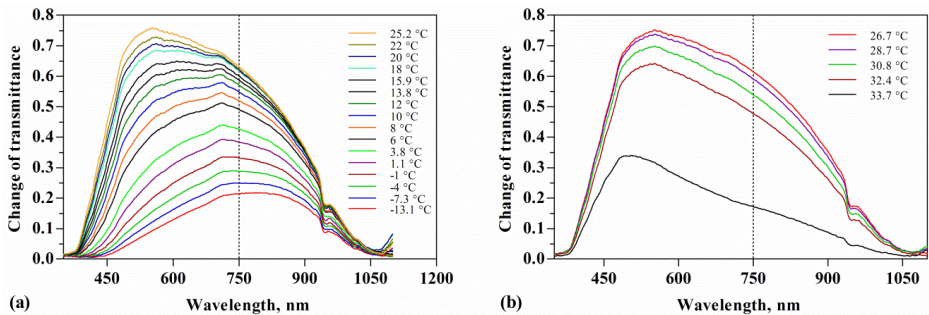


**Figure 18.** Change of transmittance  $\Delta T$  vs. wavelength  $\lambda$  evolution with increasing temperature, a) from -13.1 °C to 25.2 °C and b) from 26.7 °C to 33.7 °C. Dotted line at 750 nm shows the approximate limit of the visible range.

Figure 19 presents the wavelength of the maximum  $\Delta T$  as a function of the temperature, represented in two different ways: as experimental maxima vs. the temperature and as maxima of the 8<sup>th</sup> degree polynomial curve, found by the standard method of least squares fitting to the experimental data points ( $\Delta T$  vs.  $\lambda$  curves at different temperatures) vs. the temperature. The latter provides a better description of the location of the maxima of the curve while avoiding the local deviations.

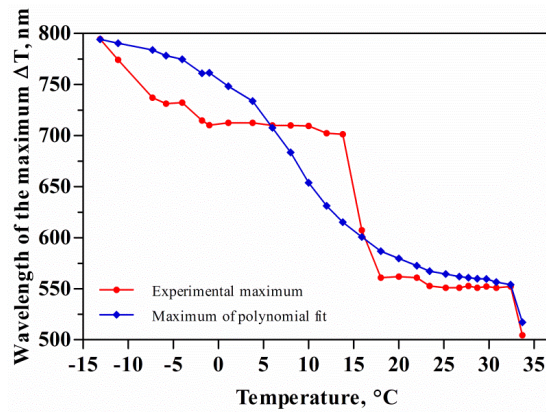


**Figure 19.** Wavelength of the maximum of  $\Delta T$  vs.  $\lambda$  curve as a function of temperature. Similarly to Figure 18, the maximum of  $\Delta T$  vs.  $\lambda$  shifts toward shorter wavelengths during the evolution with increasing voltage (at a temperature 25.2 °C) (Figure 20).

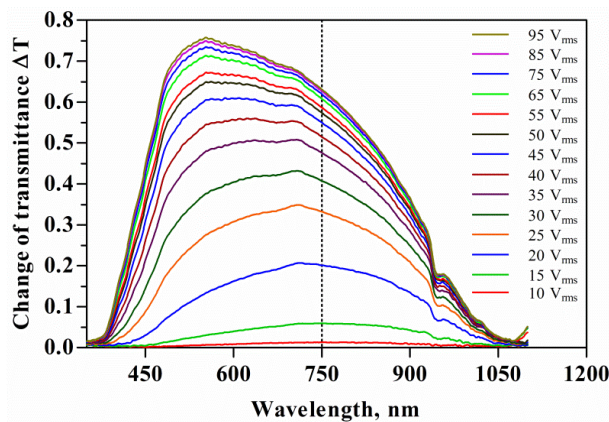


**Figure 20.**  $\Delta T$  vs.  $\lambda$  evolution with increasing voltage at temperature 25.2 °C.

At low voltages, the strongest electro-optical effect occurs at the visible-IR boundary, and it gradually moves toward the middle of the visible range as the voltage is increased to  $95 V_{\text{rms}}$ , for which  $\Delta T$  achieves its maximum (75.9%) at 551 nm. It can be concluded from Figures 18 and 20 that the main effect of the increasing temperature is a decrease in the operating voltage. The shift of the maximum toward shorter wavelengths with increasing voltage could have several possible explanations. It is possible that in larger droplets, which are responsible for effective scattering at longer wavelengths, the change in the liquid crystal effective refractive index is induced at lower voltages (i.e., the liquid crystal molecules tend to align parallel to the electric field in weaker electric fields). Thus, larger droplets may not contribute significantly to the further increase of the transmittance as voltage is increased. It is also possible that several director field configurations occur as electric field is gradually increased. This is evident under a polarized optical microscope as changes in a droplet are observable over a wide applied voltage range, indicating the rearrangement of director field from the initial configuration. Regardless of the cause, it can be said that the increasing voltage decreases the scattering cross-section.

To better compare the change of the  $\Delta T$  vs.  $\lambda$  graph with increasing temperature (Figure 18) and increasing voltage (at a constant temperature of 25.2 °C, Figure 20), the area  $S$  under the  $\Delta T$  vs.  $\lambda$  curve in the visible range is plotted as a function of temperature and voltage in (Figure 21 a) and Figure 21 b), respectively). These two graphs illustrate the quality of the GDLC electro-optical device in the full visible spectrum because they are generalizations of the transmittance vs. applied voltage curves, which are usually specified at one wavelength. The shape of the curve in Figure 21 b) resembles that of the  $T$  vs.  $U$  curve at constant wavelength. The theoretical maximum for the area  $S$  under a  $\Delta T$  vs.  $\lambda$  curve in the visible range is 400, in which case a 100% change in the transmittance occurs at all wavelengths in the visible range. From Figure 21 a), it can be observed that largest area ( $S=234.89$  nm, 58.72% of the theoretical maximum) is experimentally achieved at a temperature of 25.2 °C. Additionally,  $\Delta T_{\text{max}}$  occurred at the same temperature (Figure 16); consequently, there is a good correlation between the area under a  $\Delta T$  vs.  $\lambda$  curve and height of the curve. A prerequisite to approaching the theoretical maximum is the exact matching of the dispersion curve of the matrix with the dispersion curve of the ordinary refractive index of the liquid crystal.

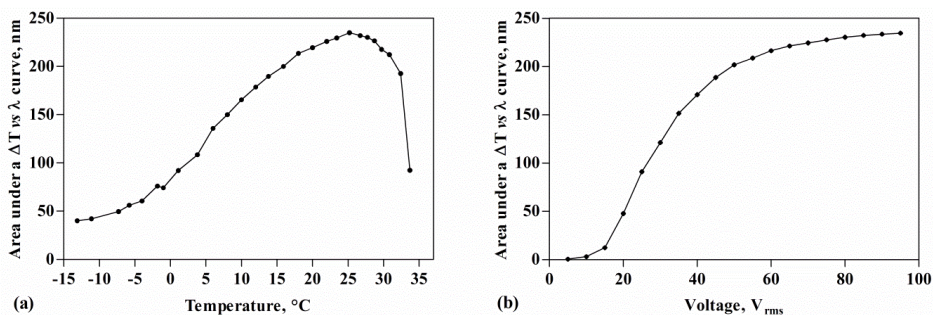


**Figure 21.** Area  $S$  under a  $\Delta T$  vs  $\lambda$  curve in visible range as a function of a) temperature and b) voltage.

### 5.3. Method of preparation of large area GDLC films (patent)

The patent that forms the part of this work focuses on the preparation method of the large area GDLC films by spraying method and can be considered *to significant extent* technical by its nature, as patents as a rule are. It became immediately clear though, as first experiments were carried out by the spraying method, that transition from spin-coating to spray-coating is not solely a technological task. As was briefly discussed in chapter 4.1, the spraying process is an important part of the synthesis due to the chemical reactions and solvent evaporation in aerosol phase. These processes complexify the film preparation but as these processes are understood and precisely controlled the spray-coating method provides far greater flexibility for film deposition as compared to other deposition methods.

The nature of the invention is described in detail in the patent application [96]. In short, the invention relates to the field of chemical technology (sol-gel chemistry) and optics, more specifically to preparation of electro-optical materials with variable transmittance. The object of this invention is a method of preparation of coating of electrically variable transmittance, which involves dispersing of liquid crystal droplets in hydrolyzable and polymerizable precursors (alkoxides) and which is applicable for preparation of electro-optical coating and coating surfaces with different shape. Described method combines preparation of surface coating material of variable transmittance and applying it on a surface (for example, manufacturing of window glass of a variable transmittance), where the process of applying the material to the surface is intrinsically related to the synthesis processes of the GDLC material.

The invention describes a novel solution to the procedure of adding water and to simultaneous adding of water and catalyst to the alkoxide precursor mixture in order to obtain coatings of variable transmittance and describes a method for preparing coating of variable transmittance on large substrate areas.

The objective of the invention is achieved through mixing of different alkoxides, liquid crystal and an appropriate amount of solvent. After that the obtained material is sprayed through water vapor environment/atmosphere with a certain acidity on the substrate (for example, quartz, silica glass) that is coated with a layer that is electrically conductive, but transparent in the visible range. While moving through humid and acidic environment, hydrolysis and polymerization reactions of the alkoxides and evaporation of the solvents take place. These processes also continue on the surface of the substrate. In the course of spraying the carrier gas jet induces underpressure in the vessel with the prepared mixture and carries the liquid mixture along. The carrier gas may be the dry gas (for example, the pure argon or nitrogen) or some mixture of gases with certain humidity (for example, air). To improve the effectiveness of the process during the period, when the mixture has left the spraying device, but has not yet reached the surface, the mixture is exposed to radiation (e.g. ultraviolet radiation), increasing the reaction speed. The method is suitable for coating large surfaces (e.g. window glasses) with electro-optical films and also allows the preparation of electro-optical films with different patterns and shapes (e.g., ads, trademarks, decorations), using masks of corresponding shape during the film preparation process (see Figure 8).

The alkoxides, which as the result of hydrolysis and polymerization processes form a solid glass matrix, can be chosen so that the catalyst (acid) is also formed within the mixture through the hydrolysis of alkoxide compounds, i.e. in contact with water. For this purpose one of the precursor compounds used may be for example trimethylchlorosilane, which gives one mole of hydrochloric acid by the reaction of one mole of alkoxide and one mole of water. When such precursors are used the hydrolyzable and polymerizable precursors (alkoxides) come in contact with catalyzing agent as the mixture is applied onto the surface, moving through the acidic water vapor. Catalyzing acid also forms in the precursor mixture through the reaction between alkoxide(s) and water vapor. Such method of adding catalyzing acid and water in the course of preparation of the coating enables controlling the speed of alkoxide hydrolysis and polymerization processes and the relative time difference between the starting points of these processes in a wide range and thus enables tuning of the properties of obtained material (the size of liquid crystal droplets and droplet size distribution).

The liquid crystal is mixed with hydrolyzable and polymerizable precursors in two different ways. In the first case the LC is mixed as a liquid phase, i.e. homogeneous solution is obtained by mixing LC with a mixture of alkoxides and solvent at room temperature and LC microdroplets are obtained through phase separation. In the second case the liquid crystal in the form of solid particles or powder is mixed with the alkoxides. In this case the liquid crystal microdroplets in the solid form are already present in the initial mixture before spraying the material to the surface, no phase separation occurs. The second method enables selective doping of LC of matrix phase with dye molecules

without contaminating the other phase. Also, in addition to the possibility of selectively doping only one of the phases, alkoxides with much higher reactivities (higher speed of hydrolysis and polymerization) compared to those of the conventional silica compounds can be used as precursors since LC microdroplets are not obtained through phase separation.

## 6. CONCLUSIONS

Two sol synthesis routes were used in preparation of GDLC materials. **The first and the simpler route** use silicon alkoxides as precursors and is simple to carry out but possesses serious limitations and fails to yield high-performance electro-optical material. This route was explored in a first stage of experimental work. GDLC films were prepared with varied Me-TES/TEOS ratios and the possibility of preparing GDLC films without adding solvent in the sol synthesis stage was shown for the first time. Generally, avoiding solvents in the synthesis process results in wider LC droplet size distribution, increased thickness of films, and larger variation of the transmittance. The sample with the biggest change in transmittance  $\Delta T$  (at 633 nm) in series prepared with ethanol had TEOS: Me-TES ratio of 2.5:1 with change in transmittance  $\Delta T=33.9\%$ , and in series prepared without ethanol had TEOS:Me-TES ratio of 5:1 with  $\Delta T=31\%$ . Although the biggest change in transmittance occurred in the sample prepared with the use of solvent, the general trend was that samples prepared without solvent exhibited bigger changes in transmittance as compared to the samples prepared with the use of ethanol as a solvent.

Different concentration of methyl groups influence the gelation time and by that the droplet size distribution. Thus it can be concluded that the operating voltage is not directly influenced by the molar ratios of the precursor alkoxides alone but by the droplet size distribution determined by these molar ratios, and proper measures must be applied in order to synchronously control the droplet size.

It was found that LC phase separation may occur in such a way that a certain percentage of LC droplets are not completely surrounded by the xerogel matrix, but are open on the film surface, which can significantly reduce the effective thickness of the films in terms of the scattering efficiency since the open droplets are filled with the organic resin in the preparation of the electro-optical sandwich element. The resin layer is necessary to fix the second electrode, to avoid dielectric breakdowns and eliminate scattering by the surface roughness.

Generally, the prepared films exhibited poor electro-optical performance, attributable to insufficient thickness (the highest achieved thickness was 3.8  $\mu\text{m}$ ), deteriorating effect of the resin and low refractive index of the matrix.

**The second and more complicated sol synthesis route** was also explored. The GDLC film preparation process was elaborated to incorporate titanium alkoxides in the synthesis process. This enabled the adjustment of the refractive index of silica glass matrix without having destructive influence on the macroscopic liquid crystal phase separation at the same time. The consequent increase in the refractive index of the matrix enabled to meet the criterions for the high performance films. High performance thick films that exhibit remarkable 75.9% change in transmittance as an electric field is applied were prepared. It was demonstrated for the first time that the crack-free thick (11.98  $\mu\text{m}$ ) GDLC films

can be successfully prepared. The absence of cracking can be attributed to the deformability of the liquid phase that prevents the stress buildup. Oblate spheroid shape of LC droplets inside the xerogel matrix was shown for the first time, indicating the possibility to control the shape of the droplets and showing the superiority of the GDLC preparation method against the PDLC preparation method in this aspect.

**An original setup was developed** that enables measurements of the transmittance dependence on applied voltage at different temperatures in full visible and near-IR spectral range. For the first time change of transmittance vs. light wavelength was measured for a GDLC film at different temperatures, showing the distinct maxima in the mid-visible range. Transmittance vs. applied voltage measurements at different temperatures demonstrate the electro-optical effects at least down to  $-13\text{ }^{\circ}\text{C}$ , indicating a significant  $35.5\text{ }^{\circ}\text{C}$  reduction from the solid-nematic phase transition temperature in the macroscopic volume. This is an important property in terms of practical applications.

The area under the  $\Delta T$  vs.  $\lambda$  curve in the visible range as a function of the temperature and/or voltage was found to provide a generalized description of the electro-optical quality of the gel-glass dispersed liquid crystal films. The prepared film possessed 58.72% of the theoretical maximum area under a  $\Delta T$  vs.  $\lambda$  curve. The maximum of the curve increased and moved from the IR to the mid-visible range with increasing temperature, achieving its maximum (largest electro-optical effect) at  $25.2\text{ }^{\circ}\text{C}$  and  $551\text{ nm}$ .



## SUMMARY

Gel-glass dispersed liquid crystals (GDLCs) are electro-optical composite materials prepared by a sol-gel method, consisting of liquid crystal microdroplets encapsulated in inorganic or organically modified silica or mixed oxide matrices. This type of material was first prepared in 1991 and is since then very little researched with less than 20 scientific papers published in the field. The material possesses electric field dependent reversible scattering behavior and can be switched from an opaque scattering state to a transparent non-scattering state. Despite the great commercial potential as a smart window technology no commercial applications exist so far for GDLCs. The reasons behind that for short are the absence of method to prepare large area films and poor electro-optical performance.

The general goal of this work is to expand the understanding of the formation processes of GDLCs, influence of different parameters on the properties of GDLCs and electro-optical characterization of such composite materials, which is necessary in order to move closer to the industrial applicability of GDLC materials as a smart window technology. The tasks include the investigation of the possibilities of preparing (both in terms of synthesis and deposition) thick, crack-free, large area, high-performance GDLC films.

Several strategies for sol synthesis were explored to investigate the influence of different degrees of organic modification and to prepare GDLC films with high refractive index matrix. Sol synthesis process was elaborated to incorporate titanium alkoxide in the synthesis process. This enabled the adjustment of the refractive index of silica glass matrix to match the ordinary refractive index of the LC, which satisfied the important criteria for high performance films and was achieved without having destructive influence on macroscopic liquid crystal phase separation at the same time. High performance thick films that exhibit 75.9% change in transmittance as an electric field is applied were prepared. This performance is sufficient for practical applications. It was demonstrated for the first time that crack-free thick (11.98  $\mu\text{m}$ ) GDLC films can be successfully prepared. The absence of cracking can be attributed to the deformability of the liquid phase that prevents stress buildup. An original setup was developed that enables measurements of transmittance dependence on applied voltage at different temperatures in full visible and near-IR spectral range. For the first time, function of change of transmittance vs. wavelength of light at different temperatures was measured for a GDLC film, showing the distinct maxima in the mid-visible range which is the result of precise optimization of film preparation process. The prepared film possessed 58.72% of the theoretical maximum area under a  $\Delta T$  vs.  $\lambda$  curve, which was found to provide a generalized description of the electro-optical quality of the gel-glass dispersed liquid crystal films. The maximum of the curve increased and moved from the IR to the mid-visible range with increasing temperature, achieving its maximum (largest electro-optical effect) at 25.2 °C and 551 nm.

Method of preparation of large area GDLC films was elaborated and patented.

## SUMMARY IN ESTONIAN

### Hübriidsete elektrooptiliste materjalide välja töötamine ja karakteriseerimine

Geel-klaas disperseeritud vedelkristallid (GDLCs) on sool-geel meetodil valmistatavad elektrooptilised komposiitmaterjalid, mis koosnevad orgaaniliselt modifitseeritud ränioksiid- või seguoksiidmaatriksist ja selle sisse disperseeritud vedelkristalli mikrotilkadest. Sellist materjali valmistati esmakordselt 1991. aastal, millest alates on seda materjali väga vähe uuritud – ilmunud on vähem kui 20 teadusartiklit. GDLC materjali hajutavust on võimalik pööratavalt muuta ning materjali on võimalik elektrivälja abil lülitada valgust hajutava ja läbilaskva oleku vahel. Hoolimata suurest kaubanduslikust potentsiaalist muudetava läbilaskvusega aknaklaaside turul GDLC materjalil senimaani tööstuslikult ei toodeta. Põhjuseks on meetodi puudumine suure pindalaga kilede valmistamiseks ning ebapiisav läbilaskvuse muutus elektrilise pinge rakendamisel.

Antud töö üldine eesmärk on avardada arusaamist GDLC materjali formeerumise protsessidest, erinevate parameetrite mõju uurimine materjali omadustele ning materjali elektrooptiline karakteriseerimine, mis on vajalikud liikumaks lähemale GDLC materjalide tööstuslikule tootmisele ning rakendamisele muudetava läbilaskvusega akendena. Sobivus praktilisteks rakendusteks eeldab sünteesi- ja kilede sadestamisprotsesside väljatöötamist, mis võimaldaks valmistada suure pindalaga, paksud (ca. 12–15  $\mu\text{m}$ ), pragudeta ja kõrgefektiivsed GDLC kiled.

Kasutati mitut erinevat strateegiat soolide sünteesiks eesmärgiga uurida erineva orgaaniliste rühmade kontsentratsiooni mõju kile omadustele ja valmistada kõrge murdumisnäitajaga maatriksmaterjaliga GDLC kiled. Töötati välja sooli sünteesiprotokoll, mis võimaldab kasutada titaani alkoksiidi ning seeläbi tõsta GDLC maatriksi murdumisnäitajat võrdseks kasutatud vedelkristalli vastava murdumisnäitaja väärtusega, seejuures vedelkristalli makroskoopilist faasieraldust rikkumata. See omakorda võimaldas täita olulise kriteeriumi kõrgefektiivse GDLC valmistamiseks. Valmistati kiled, mille läbilaskvuse muutus elektrilise pinge rakendamisel on 75.9%, olles piisav praktilisteks rakendusteks. Esmakordselt näidati paksude (11.98  $\mu\text{m}$ ) pragudevabade GDLC kilede valmistamise võimalikkust. Pragude puudumine on seletatav vedelkristalli mikrotikade kuju muutumisega kile kuivamisel, mis takistab mehaaniliste pingetel kriitilise väärtuse ületamist. Konstrueeriti originaalne katseseade, mis võimaldab läbilaskvuse pingesõltuvuse mõõtmist erinevatel temperatuuridel nähtavas ja lähi-infrapunases spektriosas. Esmakordselt mõõdeti läbilaskvuse muutuse sõltuvus lainepikkusest laias temperatuuride vahemikus ning näidati funktsiooni  $\Delta T$  vs.  $\lambda$  maksimumi langemist nähtava lainepikkuste piirkonna keskele, mis on materjali valmistamisprotsessi täpse optimeerimise tulemus. Leiti, et  $\Delta T$  vs.  $\lambda$  sõltuvuse joonealne pindala on suurus, mis kirjeldab hästi GDLC kile elektrooptilist kvaliteeti võttes arvesse kile hajutavusomadused laias spektri-

vahemikus. Valmistatud kile  $\Delta T$  vs.  $\lambda$  sõltuvuse joonealune pindala moodustas 58.72% teoreetilisest maksimumist. Sõltuvuse maksimum suurenes temperatuuri kasvades ning liikus lähi-infrapunasest piirkonnast nähtava lainepikkuste piirkonna keskele saavutades maksimumi temperatuuril 25.2 °C ja lainepikkusel 551 nm.

Töötati välja ning patenteeriti meetod suure pindalaga GDLC kilede valmistamiseks.

## REFERENCES

- [1] P. Malik, K.K. Raina, *Opt. Mater.* 27 (2004) 613–617
- [2] J.-H. Ryu, Y.-H. Choi, K.-D. Suh, *Colloids Surf., A* 275 (2006) 126–132
- [3] K.K. Raina, P. Kumar, P. Malik, *Bull. Mater. Sci.* 29 (2006) 599–603.
- [4] L. Petti, P. Mormile, W.J. Blau, *Opt. Laser Eng.* 39 (2003) 369–377
- [5] O.V. Yaroshchuk, L.O. Dolgov, *Opt. Mater.* 29 (2007) 1097–1102
- [6] J. Bouclé, A. Kassiba, J. Emery, I.V. Kityk, M. Makowska-Janusik, J. Sanetra, N. Herlin-Boime, M. Mayne, *Phys. Lett. A* 302 (2002) 196–202
- [7] M. Zayat, D. Levy, *J. Mater. Chem.* 15 (2005) 3769–3775
- [8] D. Levy, *Pure Appl. Opt.* 5 (1996) 621–629
- [9] M. Zayat, D. Levy, *Chem. Mater.* 15 (2003) 2122–2128
- [10] N. Kejalakshmy, K. Srinivasan, *J. Phys. D: Appl. Phys.* 36 (2003) 1778–1782
- [11] D. Filipovic, P. Osmokrovic, Z. Lazarevic, *Mater. Sci. Forum* 413 (2003) 197–200
- [12] J. Lanzo, F. P. Nicoletta, G. De Filpo, G. Chidichimo, *Appl. Phys. Lett.* 74 (1999) 2635–2637
- [13] G. De Filpo, J. Lanzo, F. P. Nicoletta, G. Chidichimo, *J. Appl. Phys.* 85 (1999) 2894–2898
- [14] J. Lanzo, F.P. Nicoletta, G. De Filpo, G. Chidichimo, *J. Appl. Phys.* 92 (2002) 4271–4275
- [15] J. Lanzo, M. De Benedittis, B.C. De Simone, G. Chidichimo, *Mater. Lett.* 61 (2007) 3349–3351
- [16] J. Lanzo, M. De Benedittis, B.C. De Simone, D. Imbardelli, P. Formoso, S. Manfredi G. Chidichimo, *J. Mater. Chem.* 17 (2007) 1412–1415
- [17] N.A. Davidenko, N.A. Derevyanko, A.A. Ishchenko, V.A. Pavlov, *Opt. Spectrosc.* 91 (2001) 586–592.
- [18] Y. Iwaki, N. Ohta, *Chem. Lett.* 29 (2000) 894–895
- [19] G.A. Niklasson, C.G. Granqvist, *J. Mater. Chem.* 17 (2007) 127–156
- [20] S.-J. Yoo, J.-W. Lim, Y.-E. Sung, *Sol. Energy Mater. Sol. Cells* 90 (2006) 477–484
- [21] J.L. Fergason, *SID Int. Symp. Digest Technol. Papers* 16 (1985) 68–70.
- [22] L. Lucchetti, F. Simoni, *J. Appl. Phys.* 88 (2000) 3934–3940
- [23] W. Lee C.-C. Lee, *Nanotechnology* 17 (2006) 157–162
- [24] T. Schneider, F. Nicholson, A. Khan, J.W. Doane, L.-C. Chien, *SID Int. Symp. Digest Technol. Papers* 36 (2005) 1568–1572
- [25] G. Sumana, K.K. Raina, *J. Appl. Polym. Sci.* 94 (2004) 159–166
- [26] R. Karapinar, M. O'Neill, M. Hird, *J. Phys. D: Appl. Phys.* 35 (2002) 900–905
- [27] S. Chandrasekhar, *Liquid crystals* (Cambridge University Press, Cambridge, Great Britain, 1992)
- [28] S. Kumar, *Liquid crystals: experimental study of physical properties and phase transitions* (Cambridge University Press, Cambridge, Great Britain, 2000)
- [29] [http://www.nhk.or.jp/strl/open98/4-5/fig\\_pdlc-e.jpg](http://www.nhk.or.jp/strl/open98/4-5/fig_pdlc-e.jpg)
- [30] P. Kumar, K.K. Raina, *Curr. Appl. Phys.* 7 (2007) 636–642
- [31] P. Drzaic, *J. Appl. Phys.* 60 (1986) 2142–2148.
- [32] S. Mias, H. Camon, *J. Micromech. Microeng.* 18 (2008) 083002.
- [33] K. Takizawa, T. Fujii, M. Kawakita, H. Kikuchi, H. Fujikake, M. Yokozawa, A. Murata, K. Kishi, *Appl. Opt.* 36 (1997) 5732–5747.
- [34] B.-G. Wu, J.L. West, J.W. Doane, *Appl. Phys.* 62 (1987) 3295–3931.

- [35] G. Sumana, K.K. Raina, *Curr. Appl Phys.* 5 (2005) 277–284
- [36] S. Sakka, M. Langlet, and K. Kamiya: Handbook of sol-gel science and technology: processing, characterization and applications, Vol. 1, (Kluwer Academic Publishers, Norwell, USA 2005)
- [37] J. Livage, D. Ganguli, *Sol. Energy Mater. Sol. Cells* 68 (2001) 365–381
- [38] K. Nakanishi, *J. Porous Mater.* 4 (1997) 67–112
- [39] L.L. Hench, J.K. West, *Chem. Rev.* 90 (1990) 33–72
- [40] N.Y. Turova (editor), E. P. Turevskaya (editor), V.G. Kessler (editor), M. I. Yanovskaya (editor): The Chemistry of Metal Alkoxides (Kluwer Academic Publishers, Dordrecht, 2002), Ch. 9
- [41] G.W. Scherer, *J. Am. Ceram. Soc.* 73 (1990) 3–14
- [42] G.W. Scherer, *J. Non-Cryst. Solids* 147–148 (1992) 363–374
- [43] M.J. Mosquera, M. Bejarano, N. de la Rosa-Fox, L. Esquivias, *Langmuir* 19 (2003) 951–957
- [44] L. Hench, D.R. Ulrich: Science of Ceramic Chemical Processing (Wiley, New York, 1986)
- [45] H. Shiomi, C. Kakimoto, A. Nakahira, *J. Sol-gel Sci. Technol.* 19 (2000) 759–763
- [46] J.H. Harreld, T. Elbina, N. Tsubo, G. Stucky, *J. Non-Cryst. Solids* 298 (2002) 241–251.
- [47] C.J. Brinker, G.W. Scherer, Sol-gel science, the physics and chemistry of sol-gel processing (Academic Press, Boston, 1990)
- [48] M.J. Mosquera, D.M. de los Santos, L. Valdez-Castro, L. Esquivias, *J. Non-Cryst. Solids* 354 (2008) 645–650
- [49] H. Kozuka, A. Higuchi, *J. Am. Ceram. Soc.* 86 (1) (2003) 33–38
- [50] M. Yoshida, P.N. Prasad, *Chem. Mater.* 8 (1996) 235–241
- [51] S. Sakka, *J. Sol-Gel Sci. Technol.* 26 (2003) 29–33
- [52] J.D. Mackenzie, *J. Sol-Gel Sci. Technol.* 26 (2003) 23–27
- [53] H. Schmidt, *J. Non-Crystalline Solids* 73 (1985) 681–691
- [54] F. Mammeri, E. Le Bourhis, L. Rozes, C. Sanchez, *J. Mater. Chem.* 15 (2005) 3787–3811
- [55] G. Kickelbick (editor), Hybrid materials (Wiley-VCH, Weinheim, Germany, 2007) Ch. 1
- [56] J. Wen, G.L. Wilkes, *Chem. Mater.* 8 (1996) 1667–1681
- [57] U. Schubert, N. Hüsing, A. Lorenz, *Chem. Mater.* 7 (1995) 2010–2027
- [58] J. Malzbender, J.M.J. den Toonder, A.R. Balkenende, G. de With, *Mater. Sci. Eng. R* 36 (2002) 47–103
- [59] Y. Xu, D. Wu, Y. H. Sun, Z. H. Li, B. Z. Dong, Z. H. Wu, *J. Non-Cryst. Solids* 351 (2005) 258–266
- [60] S.S. Latthe, S.L. Dhere, C. Kappenstein, H. Imai, V. Ganesan, A. Venkateswara Rao, P.B. Waghe, S.C. Gupta, *Appl. Surf. Sci.* 256 (2010) 3259–3264
- [61] H. Xie, J. Wei, X. Zhang, *Journal J. Phys. Conf. Ser.* 28 (2006) 95–99.
- [62] D. Avnir, D. Levy, R. Reisfeld, *J. Phys. Chem.* 88 (1984) 5956–5959
- [63] Y. Dimitriev, Y. Ivanova, R. Iordanova, *J. Univ. Chem. Technol. Metallurgy*, 43 (2) (2008) 181–192
- [64] P.T. Tanev, M. Chibwe, T.J. Pinnavaia, *Nature* 368 (1994) 321–323
- [65] R.M. Almeida, S. Portal, *Curr. Opin. Solid State Mater. Sci.* 7 (2003) 151–157
- [66] R.M. De Vos, H. Verweij, *Science* 279 (1998) 1710–1711
- [67] J. Sekulić, J.E. ten Elshof, D.H.A. Blank, *J. Membr. Sci.* 254 (2005) 267–274
- [68] R. Baetens, B.P. Jelle, A. Gustavsen, *Energy Build.* 43 (2011) 761–769

- [69] S.-H. Wang, T.-C. Choua, C.-C. Liu, *Sens. Actuators, B* 94 (2003) 343–351
- [70] M.M. Yusuf, H. Imai, H. Hirashima, *J. Non-Cryst. Solids* 285 (2011) 90–95
- [71] A. Imhof, D.J. Pine, *Nature* 389 (1997) 948–951
- [72] A. Stein, *Microporous Mesoporous Mater.* 44–45 (2001) 227–239
- [73] K. Nakanishi, N. Tanaka, *Acc. Chem. Res.* 40 (2007) 863–873
- [74] K. Nakanishi, N. Soga, *J. Am. Ceram. Soc.* 74 (1991) 2518–2530
- [75] K. Nakanishi, *Bull. Chem. Soc. Jpn.* 79 (2006) 673–691
- [76] K. Wongcharee, M. Brungs, R. Chaplin, Y.J. Hong, E. Sizgek, *J. Sol-Gel Sci. Technol.* 29 (2004) 115–124
- [77] J.M. Otón, A. Serrano, C. J. Cerna, D. Levy, *Liq. Cryst.* 5 (1991) 733–739
- [78] D. Levy, C.J. Serna, J.M. Otón, *Mater. Lett.* 10 (1991) 470–476.
- [79] A. Nath, P. Mandal, S. Paul, B. Chaudhury, *Mol. Cryst. Liq. Cryst.* A 281 (1996) 57–63
- [80] P.G. Cummins, D.A. Dunmur, D.A. Laidler, *Mol. Cryst. Liq. Cryst.* 30 (1975) 109–121
- [81] J. Li, C.-H. Wen, S. Gauza, R. Lu, S.-T. Wu, *IEEE/OSA J. Disp. Technol.* 1(1) (2005) 51–61
- [82] M. Timusk, M. Järvekülg, R. Lõhmus, I. Kink, and K. Saal, *Mater. Sci. Eng., B* 172 (2010) 1–5
- [83] W.-P. Chang, W.-T. Whang, J.-C. Wong, *Jpn. J. Appl. Phys., Part 1* 34 (1995) 1888–1894
- [84] M. Timusk, M. Järvekülg, A. Salundi, R. Lõhmus, S. Leinberg, I. Kink, K. Saal, *J. Mater. Res.* 27(9) (2012) 1257–1264
- [85] E. Castellón, M. Zayat, D. Levy, *Phys. Chem. Chem. Phys.* 11 (2009) 6234–6241
- [86] J.M. Otón, J. M. S. Pena, A. Serrano, *Appl. Phys. Lett.* 66 (1995) 929–931
- [87] P.S. Drzaic, *Liquid Crystal Dispersions*. (World Scientific, Teaneck, USA, 1995)
- [88] O.O. Prischepa, A.V. Shabanov, V.Ya. Zyryanov, *Mol. Cryst. Liq. Cryst.* 438 (2005) 141–150
- [89] Y.-Y. Huang, K.-S. Chou, *Ceram. Int.* 29 (2003) 485–493
- [90] K. Vorotilov, V. Petrovsky, V. Vasiljev, *J. Sol-Gel Sci. Technol.* 5 (1995) 173–183
- [91] J. McKibben, M. Paradi P. Haaland, *Proceedings of the Display Manufacturing Technology Conference (San Jose: SID, 1995)*, pp. 79–81
- [92] D. Levy, A. Serrano, J.M. Otón, *J. Sol-Gel Sci. Technol.* 2 (1994) 803–807
- [93] M. Hori, M. Toki, *J. Sol-Gel Sci. Technol.* 19 (2000) 349–352
- [94] I. Oja, A. Mere, M. Krunks, R. Nisumaa, C.-H. Solterbeck, M. Es-Souni, *Thin Solid Films* 515 (2006) 674–677
- [95] M. Kobayashi, T.R. Olding, M. Sayer, C.-K. Jen, *Ultrasonics* 39 (2002) 675–680
- [96] M. Timusk, M. Järvekülg, K. Saal, R. Lõhmus, I. Kink, A. Lõhmus (University of Tartu, Estonia; Estonian Nanotechnology Competence Centre), „Method of preparation of surface coating of variable transmittance and electro-optical appliance including the same “ *patent application* WO 2010108987 (2010).
- [97] U. Schubert, *J. Mater. Chem.* 15 (2005) 3701–3715
- [98] K.M. Hung, C.S. Hsieh, W.D. Yang, H.J. Tsai, *J. Electron. Mater.* 36 (2007) 245–252
- [99] A. Leautic, F. Babonneau, J. Livage, *Chem. Mater.* 1(2) (1989) 240–247

- [100] A. Sadeghzadeh Attar, M. Sasani Ghamsari, F. Hajiesmaeilbaigi, Sh. Mirdamadi, K. Katagiri, K. Koumoto, *J. Phys. D: Appl. Phys.* 41 (2008) 155318
- [101] J. Ren, Z. Li, S. Liu, Y. Xing, and K. Xie, *Catal. Lett.* 124 (2008) 185–194
- [102] R. Swanepoel, *J. Phys. E: Sci. Instrum.* 16 (1983) 1214–1222
- [103] X. Zhang, H. Lu, A.M. Soutar, X. Zeng, *J. Mater. Chem.* 14 (2004) 357–361
- [104] M. Boussoualem, F. Roussel, M. Ismaili, *Phys. Rev. E* 69 (2004) 031702
- [105] F.M. Aliev, *J. Non-Cryst. Solids.* 489 (2002) 307–310
- [106] F.P. Nicoletta, M. Caporusso, H.-A. Hakemi, G. Chidichimo, *Mol. Cryst. Liq. Cryst. Sci. Technol., Sect. A* 336 (1999) 83–91

## **ACKNOWLEDGEMENTS**

I am grateful to all the people who, knowingly or unknowingly had positive influence for the completion of this work.

Special thanks to my supervisors Rünno Lõhmus and Kristjan Saal for support and for bringing me into this interesting topic. Also, I would like to thank colleagues whose help I appreciate greatly: Martin Järvekülg, Aigi Salundi, Silver Leinberg, Ants Lõhmus, Ilmar Kink, Jörgen Metsik, Madis Lobjakas, Fredrik Punga, Uno Mäeorg, Madis Paalo, Tanel Tätte, Aarne Kasikov, Siim Pikker and Kadri Savi.

I would like to emphasize the importance of Estonian Nanotechnology Competence Center for providing financial support and making this project possible in its current form.

This work was supported by Estonian Science Foundation grants no. 8428, 8420 and 9007, by the European Eurocores project “Nanoparma” and Graduate School on Functional Materials and Technologies, EU Social Funds project 1.2.0401.09-0079. This study was also supported by the European Union through the European Regional Development Fund (Centre of Excellence “Mesosystems: Theory and Applications”, TK114).



## **PUBLICATIONS**

# **CURRICULUM VITAE**

**Martin Timusk**

## **General data**

Date and place of birth 27. February 1984, Tartu  
Citizenship Estonian  
Contact Institute of Physics, University of Tartu  
Riia 142, 51014 Tartu  
Phone +372 5340 1774  
E-mail martin.timusk@ut.ee

## **Education**

2007–2012 University of Tartu, PhD Student (physics)  
2005–2007 University of Tartu, MSc (physics)  
2002–2005 University of Tartu, BA (physics)  
1999–2002 Põltsamaa Ühisgümnaasium

## **Language skills**

Estonian mother tongue  
English good in speaking and writing  
Russian basics

## **Professional employment**

2007–... Institute of Physics, University of Tartu, engineer  
2006–... Estonian Nanotechnology Competence Center

## **Supervised dissertations**

2009 Lauri Kaldamäe, BA in physics  
2010 Kadri Savi, BA in physics  
2011 Lauri Kaldamäe, MSc in physics  
Currently under supervision: Jörgen Metsik, MSc in chemistry

## **Awards**

2010 Estonian Physical Society student award.

# ELULOOKIRJELDUS

## Martin Timusk

### Üldinfo

Sünniaeg ja -koht 27.veebbruar 1984, Tartu  
kodakondsus Eesti  
Kontaktandmed Tartu Ülikooli Füüsika Instituut  
Riia 142, 51014 Tartu  
Telefon +372 5340 1774  
E-mail martin.timusk@ut.ee

### Haridus

2007–2012 Tartu Ülikool, doktoriõpe (füüsika)  
2005–2007 Tartu Ülikool, magistriõpe (füüsika)  
2002–2005 Tartu Ülikool, bakalaureuseõpe (füüsika)  
1999–2002 Põltsamaa Ühisgümnaasium

### Keeleoskus

eesti keel emakeel  
inglise keel hea kirjas ja kõnes  
vene keel baasteadmised

### Teenistuskäik

2007–... Tartu Ülikooli Füüsika Instituut, insener  
2006–... Eesti Nanotehnoloogiarenduskeskuse AS

### Juhendatud lõputööd

2009 Lauri Kaldamäe, bakalaureusetöö füüsikas  
2010 Kadri Savi, bakalaureusetöö füüsikas  
2011 Lauri Kaldamäe, magistrیتöö füüsikas  
Praegu juhendamisel: Jörgen Metsik, magistrیتöö keemias

### Auhinnad

2010 Eesti Füüsika Seltsi üliõpilaspreamia

## DISSERTATIONES PHYSICAE UNIVERSITATIS TARTUENSIS

1. **Andrus Ausmees.** XUV-induced electron emission and electron-phonon interaction in alkali halides. Tartu, 1991.
2. **Heiki Sõnajalg.** Shaping and recalling of light pulses by optical elements based on spectral hole burning. Tartu, 1991.
3. **Sergei Savihhin.** Ultrafast dynamics of F-centers and bound excitons from picosecond spectroscopy data. Tartu, 1991.
4. **Ergo Nõmmiste.** Leelishalogeniidide röntgenelektronemissioon kiiritamisel footonitega energiaga 70–140 eV. Tartu, 1991.
5. **Margus Rätsep.** Spectral gratings and their relaxation in some low-temperature impurity-doped glasses and crystals. Tartu, 1991.
6. **Tõnu Pullerits.** Primary energy transfer in photosynthesis. Model calculations. Tartu, 1991.
7. **Olev Saks.** Attoampri diapsoonis voolude mõõtmise füüsikalised alused. Tartu, 1991.
8. **Andres Virro.** AlGaAsSb/GaSb heterostructure injection lasers. Tartu, 1991.
9. **Hans Korge.** Investigation of negative point discharge in pure nitrogen at atmospheric pressure. Tartu, 1992.
10. **Jüri Maksimov.** Nonlinear generation of laser VUV radiation for high-resolution spectroscopy. Tartu, 1992.
11. **Mark Aizengendler.** Photostimulated transformation of aggregate defects and spectral hole burning in a neutron-irradiated sapphire. Tartu, 1992.
12. **Hele Siimon.** Atomic layer molecular beam epitaxy of  $A^2B^6$  compounds described on the basis of kinetic equations model. Tartu, 1992.
13. **Tõnu Reinot.** The kinetics of polariton luminescence, energy transfer and relaxation in anthracene. Tartu, 1992.
14. **Toomas Rõõm.** Paramagnetic  $H^{2-}$  and  $F^+$  centers in CaO crystals: spectra, relaxation and recombination luminescence. Tallinn, 1993.
15. **Erko Jalviste.** Laser spectroscopy of some jet-cooled organic molecules. Tartu, 1993.
16. **Alvo Aabloo.** Studies of crystalline celluloses using potential energy calculations. Tartu, 1994.
17. **Peeter Paris.** Initiation of corona pulses. Tartu, 1994.
18. **Павел Рубин.** Локальные дефектные состояния в  $CuO_2$  плоскостях высокотемпературных сверхпроводников. Тарту, 1994.
19. **Olavi Ollikainen.** Applications of persistent spectral hole burning in ultrafast optical neural networks, time-resolved spectroscopy and holographic interferometry. Tartu, 1996.
20. **Ülo Mets.** Methodological aspects of fluorescence correlation spectroscopy. Tartu, 1996.
21. **Mikhail Danilkin.** Interaction of intrinsic and impurity defects in CaS:Eu luminophors. Tartu, 1997.

22. **Ирина Кудрявцева.** Создание и стабилизация дефектов в кристаллах KBr, KCl, RbCl при облучении ВУФ-радиацией. Тарту, 1997.
23. **Andres Osvet.** Photochromic properties of radiation-induced defects in diamond. Tartu, 1998.
24. **Jüri Örd.** Classical and quantum aspects of geodesic multiplication. Tartu, 1998.
25. **Priit Sarv.** High resolution solid-state NMR studies of zeolites. Tartu, 1998.
26. **Сепрей Долгов.** Электронные возбуждения и дефектообразование в некоторых оксидах металлов. Тарту, 1998.
27. **Kaupo Kukli.** Atomic layer deposition of artificially structured dielectric materials. Tartu, 1999.
28. **Ivo Heinmaa.** Nuclear resonance studies of local structure in  $\text{RBa}_2\text{Cu}_3\text{O}_{6+x}$  compounds. Tartu, 1999.
29. **Aleksander Shelkan.** Hole states in  $\text{CuO}_2$  planes of high temperature superconducting materials. Tartu, 1999.
30. **Dmitri Nedvedrov.** Nonlinear effects in quantum lattices. Tartu, 1999.
31. **Rein Ruus.** Collapse of 3d (4f) orbitals in 2p (3d) excited configurations and its effect on the x-ray and electron spectra. Tartu, 1999.
32. **Valter Zazubovich.** Local relaxation in incommensurate and glassy solids studied by Spectral Hole Burning. Tartu, 1999.
33. **Indrek Reimand.** Picosecond dynamics of optical excitations in GaAs and other excitonic systems. Tartu, 2000.
34. **Vladimir Babin.** Spectroscopy of exciton states in some halide macro- and nanocrystals. Tartu, 2001.
35. **Toomas Plank.** Positive corona at combined DC and AC voltage. Tartu, 2001.
36. **Kristjan Leiger.** Pressure-induced effects in inhomogeneous spectra of doped solids. Tartu, 2002.
37. **Helle Kaasik.** Nonperturbative theory of multiphonon vibrational relaxation and nonradiative transitions. Tartu, 2002.
38. **Tõnu Laas.** Propagation of waves in curved spacetimes. Tartu, 2002.
39. **Rünno Lõhmus.** Application of novel hybrid methods in SPM studies of nanostructural materials. Tartu, 2002.
40. **Kaido Reivelt.** Optical implementation of propagation-invariant pulsed free-space wave fields. Tartu, 2003.
41. **Heiki Kasemägi.** The effect of nanoparticle additives on lithium-ion mobility in a polymer electrolyte. Tartu, 2003.
42. **Villu Repän.** Low current mode of negative corona. Tartu, 2004.
43. **Алексей Котлов.** Оксианионные диэлектрические кристаллы: зонная структура и электронные возбуждения. Тарту, 2004.
44. **Jaak Talts.** Continuous non-invasive blood pressure measurement: comparative and methodological studies of the differential servo-oscillometric method. Tartu, 2004.
45. **Margus Saal.** Studies of pre-big bang and braneworld cosmology. Tartu, 2004.

46. **Eduard Gerškevičs.** Dose to bone marrow and leukaemia risk in external beam radiotherapy of prostate cancer. Tartu, 2005.
47. **Sergey Shchemelyov.** Sum-frequency generation and multiphoton ionization in xenon under excitation by conical laser beams. Tartu, 2006.
48. **Valter Kiisk.** Optical investigation of metal-oxide thin films. Tartu, 2006.
49. **Jaan Aarik.** Atomic layer deposition of titanium, zirconium and hafnium dioxides: growth mechanisms and properties of thin films. Tartu, 2007.
50. **Astrid Rekker.** Colored-noise-controlled anomalous transport and phase transitions in complex systems. Tartu, 2007.
51. **Andres Punning.** Electromechanical characterization of ionic polymer-metal composite sensing actuators. Tartu, 2007.
52. **Indrek Jõgi.** Conduction mechanisms in thin atomic layer deposited films containing  $\text{TiO}_2$ . Tartu, 2007.
53. **Aleksei Krasnikov.** Luminescence and defects creation processes in lead tungstate crystals. Tartu, 2007.
54. **Küllike Rägo.** Superconducting properties of  $\text{MgB}_2$  in a scenario with intra- and interband pairing channels. Tartu, 2008.
55. **Els Heinsalu.** Normal and anomalously slow diffusion under external fields. Tartu, 2008.
56. **Kuno Kooser.** Soft x-ray induced radiative and nonradiative core-hole decay processes in thin films and solids. Tartu, 2008.
57. **Vadim Boltrushko.** Theory of vibronic transitions with strong nonlinear vibronic interaction in solids. Tartu, 2008.
58. **Andi Hektor.** Neutrino Physics beyond the Standard Model. Tartu, 2008.
59. **Raavo Josepson.** Photoinduced field-assisted electron emission into gases. Tartu, 2008.
60. **Martti Pärs.** Study of spontaneous and photoinduced processes in molecular solids using high-resolution optical spectroscopy. Tartu, 2008.
61. **Kristjan Kannike.** Implications of neutrino masses. Tartu, 2008.
62. **Vigen Issahhanjan.** Hole and interstitial centres in radiation-resistant  $\text{MgO}$  single crystals. Tartu, 2008.
63. **Veera Krasnenko.** Computational modeling of fluorescent proteins. Tartu, 2008.
64. **Mait Müntel.** Detection of doubly charged higgs boson in the CMS detector. Tartu, 2008.
65. **Kalle Kepler.** Optimisation of patient doses and image quality in diagnostic radiology. Tartu, 2009.
66. **Jüri Raud.** Study of negative glow and positive column regions of capillary HF discharge. Tartu, 2009.
67. **Sven Lange.** Spectroscopic and phase-stabilisation properties of pure and rare-earth ions activated  $\text{ZrO}_2$  and  $\text{HfO}_2$ . Tartu, 2010.
68. **Aarne Kasikov.** Optical characterization of inhomogeneous thin films. Tartu, 2010.

69. **Heli Valtna-Lukner.** Superluminally propagating localized optical pulses. Tartu, 2010.
70. **Artjom Vargunin.** Stochastic and deterministic features of ordering in the systems with a phase transition. Tartu, 2010.
71. **Hannes Liivat.** Probing new physics in  $e^+e^-$  annihilations into heavy particles via spin orientation effects. Tartu, 2010.
72. **Tanel Mullari.** On the second order relativistic deviation equation and its applications. Tartu, 2010.
73. **Aleksandr Lissovski.** Pulsed high-pressure discharge in argon: spectroscopic diagnostics, modeling and development. Tartu, 2010.
74. **Aile Tamm.** Atomic layer deposition of high-permittivity insulators from cyclopentadienyl-based precursors. Tartu, 2010.
75. **Janek Uin.** Electrical separation for generating standard aerosols in a wide particle size range. Tartu, 2011.
76. **Svetlana Ganina.** Hajusandmetega ülesanded kui üks võimalus füüsika-õppe efektiivsuse tõstmiseks. Tartu, 2011
77. **Joel Kuusk.** Measurement of top-of-canopy spectral reflectance of forests for developing vegetation radiative transfer models. Tartu, 2011.
78. **Raul Rammula.** Atomic layer deposition of  $\text{HfO}_2$  – nucleation, growth and structure development of thin films. Tartu, 2011.
79. **Сергей Наконечный.** Исследование электронно-дырочных и интерстициал-вакансионных процессов в монокристаллах  $\text{MgO}$  и  $\text{LiF}$  методами термоактивационной спектроскопии. Тарту, 2011.
80. **Niina Voropajeva.** Elementary excitations near the boundary of a strongly correlated crystal. Tartu, 2011.